

Applications of Low Dimensional Manifolds:

- 1. Resolved Viscous Detonations with Detailed H_2/O_2 Kinetics,*
- 2. Combustion of HMX or RDX Product Gases.*

by

Joseph M. Powers

Department of Aerospace and Mechanical Engineering

University of Notre Dame

presented at the

1999 Explosives Research Program Review

Los Alamos National Laboratory

Los Alamos, New Mexico

6 October 1999

Acknowledgments

Prof. Samuel Paolucci, ND-AME,

Dr. Christopher Bowman, Post-Doc, ND-AME,

Mr. Sandeep Singh, Ph.D. Candidate, ND-AME,

Mr. Yevgenii Rastigejev, Ph.D. Candidate, ND-AME,

Dr. John Liao, LANL,

Dr. John Lyman, LANL,

Dr. Steven Son, LANL.

Outline

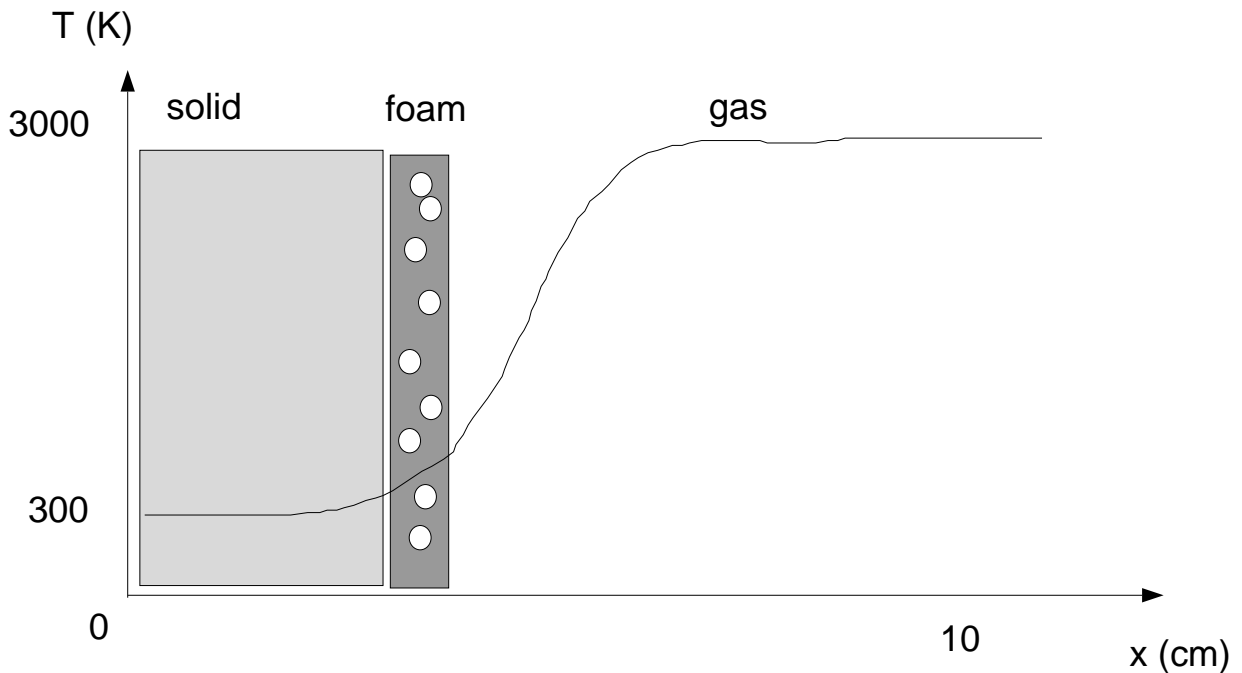
- Motivation
- Goals
- Description of ILDM technique
- Description of wavelet technique
- Detailed results for $H_2 - O_2$ detonation
- Preliminary Results for HMX combustion
- Summary

Motivation

- Detailed finite rate kinetics critical in reactive fluid mechanics:
 - Candle flames,
 - Atmospheric chemistry,
 - Internal combustion engines,
 - Gas phase reactions in energetic solid combustion.
- Common detailed kinetic models are computationally expensive.
 - 150 *hr* supercomputer time for calculation of steady, laminar, axisymmetric, methane-air diffusion flame (Smooke)
 - Expense increases with
 - * number of species and reactions modeled (linear effect),
 - * *stiffness*–ratio of slow to fast time scales, (geometric effect).
 - Fluid mechanics time scales: 10^{-5} *s* to 10^1 *s*.
 - Reaction time scales: 10^{-14} *s* to 10^2 *s*.
- Reduced kinetics necessary given current computational resources.
- Adaptive discretization necessary for fine spatial structures.
- Inclusion of *physical* diffusion necessary for *numerical* convergence.

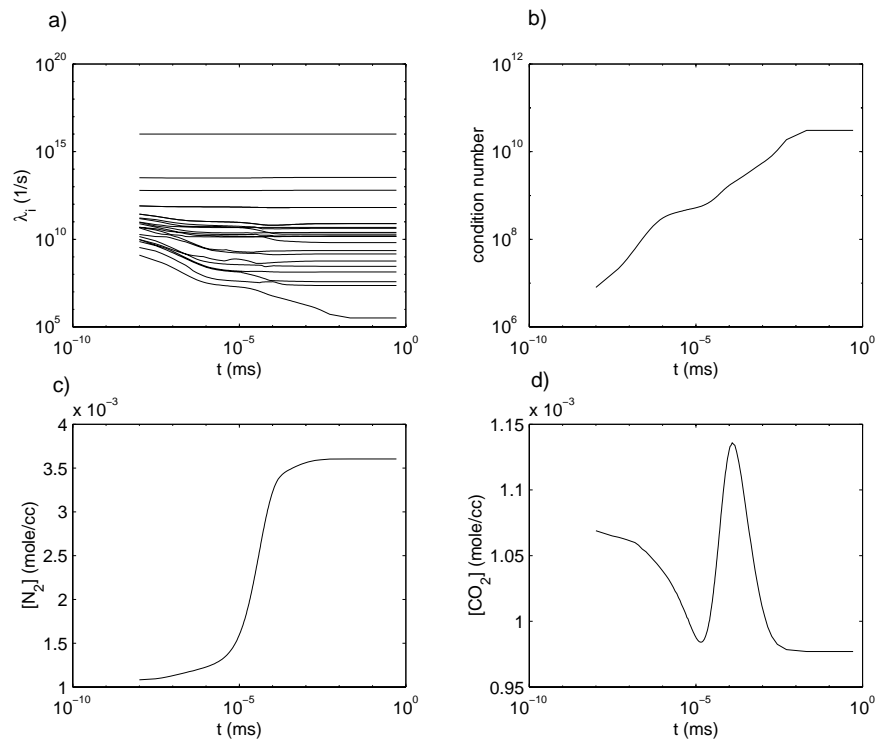
RDX/HMX COMBUSTION

- part of ongoing theoretical/experimental LANL study of low pressure $\sim 10 \text{ atm}$ combustion of explosives (Son, Liau, et al.),
- similar to solid propellant combustion,
- preheat zone in semi-infinite solid,
- two-phase bubbly liquid foam layer,
- gaseous flame region,
- gas phase reactions greatest computational burden in simulations.



RDX GAS PHASE COMBUSTION SIMULATION

- Uses Yetter's 45 species, 232 reaction detailed kinetics mechanism,
- Constant pressure
- Diffusive mass, momentum, and energy transport
- fastest time scales $\sim 10^{-16}$ s!
- stiffness ratio (fastest time scale/slowest time scale) $\sim 10^{11}$



Why Diffusion?

- Diffusion traditionally not modelled in detonation studies,
- Argued that very thin shock structures, thickness = $O(\mu m)$, will have minimal influence on reaction events,
- However, inviscid solutions to two-dimensional reactive Euler equations in mildly unstable regimes do not appear to converge, while viscous counterparts do (Singh, Powers, Paolucci, AIAA, 1999),
- Hypothesis: inherent numerical diffusion is selecting structures in “inviscid” calculations; these evolve unphysically with grid size,
- When physical diffusion zones are resolved, grid-independent physical diffusion dominates over numerical diffusion.
- Prohibitively expensive to compute simultaneous viscous and reaction zone structures with common numerical techniques and actual physical parametric values.
- SPP modelled reaction length/diffusion length ~ 10 to achieve resolved results; larger ratios necessary to model real systems.
- Adaptive wavelet collocation technique used here allows *physically correct* reaction length/diffusion length for H_2/O_2 .

Goals

- Implement robust new reduced kinetic method (Intrinsic Low Dimensional Manifold-ILDM) of Maas and Pope (1992)
- Extend ILDM method to systems with time and space dependency.
- Extend wavelet collocation technique (Paolucci & Vasilyev) to combustion systems,
- Couple wavelet and ILDM techniques.
- Applications:
 - ignition delay in shock tubes; *detailed results*,
 - multidimensional unstable viscous detonations; *preliminary results*,
 - Bunsen burner flames,
 - rocket nozzle flows,
 - HMX gas phase reactions; *joint effort with Los Alamos*.

Common Reduced Kinetics Strategies

- Fully frozen limit: no reaction allowed, *uninteresting*
- Fully equilibrated limit: commonly used in some problems
 - has value for events in which fluid time scales are slow with respect to reaction time scales,
 - misses events which happen on chemical time scales.
- Simple one and two step models
 - require significant intuition and curve fitting,
 - can give good first order results,
 - are often not robust.
- Partial equilibrium and steady-state assumptions
 - again require intuition,
 - are not robust.
- Sensitivity analysis
 - can remove need to include unimportant reactions,
 - not guaranteed to remove stiffness.

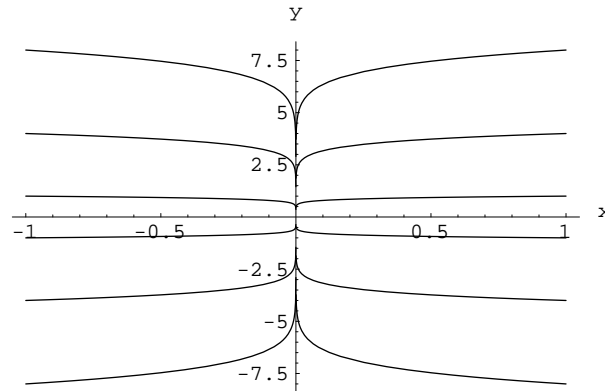
Intrinsic Low-Dimensional Manifold Method (ILDm)

- Uses a dynamical systems approach,
- Does not require imposition of *ad hoc* partial equilibrium or steady state assumptions,
- Fast time scale phenomena are systematically equilibrated,
- Slow time scale phenomena are resolved in time,
- n -species gives rise to a n -dimensional phase space (same as composition space) for isochoric, isothermal combustion in well stirred reactors,
- Identifies m -dimensional subspaces (manifolds), $m < n$, embedded within the n -dimensional phase space on which slow time scale events evolve,
 - Fast time scale events rapidly move to the manifold,
 - Slow time scale events move on the manifold.
- Computation time reduced by factor of ~ 10 for non-trivial combustion problems; manifold gives much better roadmap to find solution relative to general implicit solution techniques (Norris, 1998)

Simplest Example

$$\begin{aligned} \frac{dx}{dt} &= -10x, & x(0) &= x_o, \\ \frac{dy}{dt} &= -y, & y(0) &= y_o. \end{aligned}$$

- Stable equilibrium at $(x, y) = (0, 0)$; stiffness ratio = 10.
- ILDM is $x = 0$



- Parameterization of manifold: $x(s) = 0; y(s) = s$.

$$\frac{dy}{dt} = \frac{dy}{ds} \frac{ds}{dt}, \quad \text{chain rule}$$

$$-y(s) = \frac{dy}{ds} \frac{ds}{dt}, \quad \text{substitute from ODE and manifold}$$

$$-s = (1) \frac{ds}{dt}, \quad \text{no longer stiff!}$$

$$s = s_o e^{-t},$$

$$x(t) = 0; \quad y(t) = s_o e^{-t}.$$

- Projection onto manifold for s_o , induces small phase error.

Formulation of General Manifolds

- A well stirred chemically reactive system is modeled by a set of non-linear ordinary differential equations:

$$\frac{d\mathbf{x}}{dt} = \mathbf{F}(\mathbf{x}), \quad \mathbf{x}(0) = \mathbf{x}_o,$$

\mathbf{x} : species concentration; $\mathbf{x} \in \mathfrak{R}^n$

- Equilibrium points defined by

$$\mathbf{x} = \mathbf{x}_{eq} \text{ such that } \mathbf{F}(\mathbf{x}_{eq}) = 0.$$

- Consider a system near equilibrium (the argument can and must be extended for systems away from equilibrium) with $\tilde{\mathbf{x}} = \mathbf{x} - \mathbf{x}_{eq}$.
- Linearization gives

$$\frac{d\tilde{\mathbf{x}}}{dt} = \mathbf{F}_{\mathbf{x}} \cdot \tilde{\mathbf{x}},$$

where $\mathbf{F}_{\mathbf{x}}$ is a *constant* Jacobian matrix.

- Schur decompose the Jacobian matrix:

$$\mathbf{F}_{\mathbf{x}} = \mathbf{Q} \cdot \mathbf{U} \cdot \mathbf{Q}^T$$
$$\mathbf{Q} = \begin{pmatrix} \vdots & \vdots & & \vdots \\ q_1 & q_2 & \cdots & q_n \\ \vdots & \vdots & & \vdots \end{pmatrix}, \quad \mathbf{U} = \begin{pmatrix} \lambda_1 & u_{12} & \cdots & u_{1n} \\ 0 & \lambda_2 & \cdots & u_{2n} \\ 0 & \cdots & \ddots & \vdots \\ 0 & \cdots & 0 & \lambda_n \end{pmatrix}, \quad \mathbf{Q}^T = \begin{pmatrix} \cdots & q_1^T & \cdots \\ \cdots & q_2^T & \cdots \\ \vdots & \vdots & \vdots \\ \cdots & q_n^T & \cdots \end{pmatrix}$$

Formulation of General Manifolds (cont.)

- \mathbf{Q} is an orthogonal matrix with real Schur vectors q_i in its columns.
- \mathbf{U} is an upper triangular matrix with eigenvalues of $\mathbf{F}_{\mathbf{x}}$ on its diagonal, sometimes placed in order of decreasing magnitude.
- The Schur vectors q_i form an orthonormal basis which spans the phase space, \mathfrak{R}^n .
- We then define m slow time scales, $m \leq n$.
- Next define a non-square matrix \mathbf{W} which has in its rows the Schur vectors associated with the fast time scales:

$$\mathbf{W} = \begin{pmatrix} \cdots & \cdots & q_{m+1}^T & \cdots & \cdots \\ \cdots & \cdots & q_{m+2}^T & \cdots & \cdots \\ & & \vdots & & \\ \cdots & \cdots & q_n^T & \cdots & \cdots \end{pmatrix}.$$

- Letting the fast time scale events equilibrate defines the manifold:

$$\mathbf{W} \cdot \mathbf{F}(\mathbf{x}) = 0.$$

- If $m = 0$, no slow time scales, $\mathbf{W} = \mathbf{Q}^T$, and $\mathbf{W} \cdot \mathbf{F}(\mathbf{x}) = 0$ implies $\mathbf{Q}^T \cdot \mathbf{F}(\mathbf{x}) = 0$, implies $\mathbf{F}(\mathbf{x}) = 0$: the equilibrium point is the low dimensional manifold!

A Simple Example

- Consider

$$\begin{aligned}\frac{dx}{dt} &= -100x + y \sin y, & x(0) &= x_o, \\ \frac{dy}{dt} &= x^3 - y, & y(0) &= y_o.\end{aligned}$$

- Equilibrium points:

$$\mathbf{F} = \begin{pmatrix} 0 \\ 0 \end{pmatrix} = \begin{pmatrix} -100x + y \sin y \\ x^3 - y \end{pmatrix}, \quad \begin{pmatrix} x \\ y \end{pmatrix} = \begin{pmatrix} 0 \\ 0 \end{pmatrix}.$$

Other equilibrium points exist!

- Near the equilibrium point (0,0), linearization gives

$$\begin{pmatrix} \frac{dx}{dt} \\ \frac{dy}{dt} \end{pmatrix} = \begin{pmatrix} -100 & 0 \\ 0 & -1 \end{pmatrix} \begin{pmatrix} x \\ y \end{pmatrix},$$

which is obviously stable.

- Schur decomposition is trivial:

$$\mathbf{F}_x = \mathbf{Q} \cdot \mathbf{U} \cdot \mathbf{Q}^T$$

$$\begin{pmatrix} -100 & 0 \\ 0 & -1 \end{pmatrix} = \begin{pmatrix} 1 & 0 \\ 0 & 1 \end{pmatrix} \begin{pmatrix} -100 & 0 \\ 0 & -1 \end{pmatrix} \begin{pmatrix} 1 & 0 \\ 0 & 1 \end{pmatrix}$$

- Form the manifold:

$$\begin{aligned}\mathbf{W} &= (1 \ 0), \\ \mathbf{W} \cdot \mathbf{F}(\mathbf{x}) &= (1 \ 0) \begin{pmatrix} -100x + y \sin y \\ x^3 - y \end{pmatrix} = 0,\end{aligned}$$

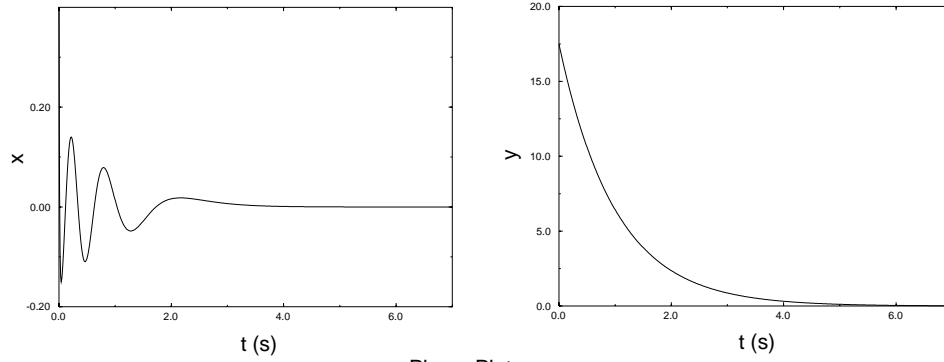
$$-100x + y \sin y = 0 \quad \text{The ILDM!}$$

A Simple Example

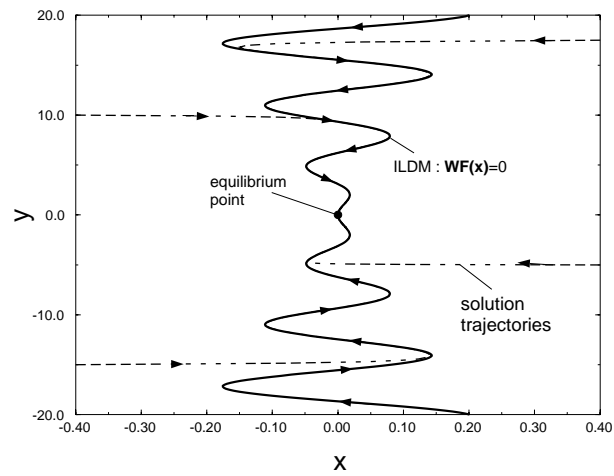
$$\frac{dx}{dt} = -100x + y \sin(y) \quad x(0) = x_0$$

$$\frac{dy}{dt} = x^3 - y \quad y(0) = y_0$$

Time Variation of X and Y



Phase Plot



Simple Example: Parameterization and Stiffness Reduction

$$\frac{dx}{dt} = -100x + y \sin y,$$
$$\frac{dy}{dt} = x^3 - y.$$

- Time scales near origin: $\tau_1 = 1.0$, $\tau_2 = 0.01$. Stiff.
- First approximation to manifold is $x = \frac{1}{100}y \sin y$.
- Parameterize manifold as

$$x = \frac{1}{100}s \sin s,$$
$$y = s.$$

- Chain rule gives

$$\frac{dy}{dt} = \frac{dy}{ds} \frac{ds}{dt}.$$

- Substitute from ODEs and parameterization:

$$x^3(s) - y(s) = \frac{dy(s)}{ds} \frac{ds}{dt},$$
$$\frac{1}{10^6} s^3 \sin^3 s - s = (1) \frac{ds}{dt},$$
$$\frac{ds}{dt} = \frac{1}{10^6} s^3 \sin^3 s - s$$

- Linearize near equilibrium at origin:

$$\frac{ds}{dt} = -s.$$

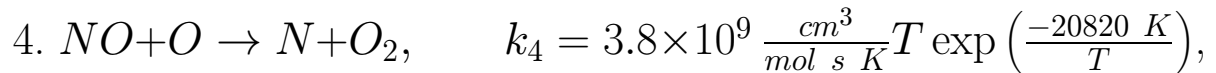
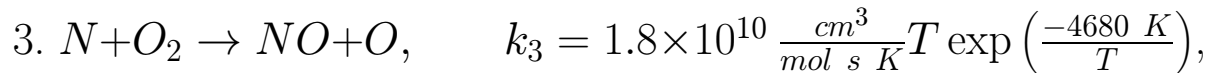
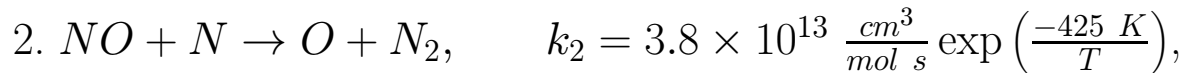
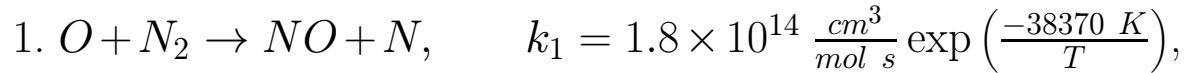
Time scale: $\tau = 1.0$ No longer stiff!

- Solve ODE for $s(t)$, substitute to get $x(s(t))$, $y(s(t))$:

$$x \sim \frac{1}{100} s_0 e^{-t} \sin(s_0 e^{-t}), \quad y \sim s_0 e^{-t}.$$

Example: Zeldovich Mechanism of NO Formation

- Mechanism (two elements, five species, two reactions):



- Take $T = 1400 \ K$, then

$$1. k_1 = 2.252 \times 10^2 \frac{cm^3}{mol \ s}$$

$$2. k_2 = 2.805 \times 10^{13} \frac{cm^3}{mol \ s}$$

$$3. k_3 = 8.905 \times 10^{11} \frac{cm^3}{mol \ s}$$

$$4. k_4 = 1.851 \times 10^6 \frac{cm^3}{mol \ s}$$

- Law of mass action for $[N_2]$, for example, gives

$$\frac{d[N_2]}{dt} = -k_1[N_2][O] + k_2[NO][N].$$

- For all species, law of mass action yields five non-linear ODEs:

$$\frac{d}{dt} \begin{pmatrix} [N] \\ [NO] \\ [N_2] \\ [O] \\ [O_2] \end{pmatrix} = \begin{pmatrix} 1 & -1 & -1 & 1 \\ 1 & -1 & 1 & -1 \\ -1 & 1 & 0 & 0 \\ -1 & 1 & 1 & -1 \\ 0 & 0 & -1 & 1 \end{pmatrix} \begin{pmatrix} k_1[N_2][O] \\ k_2[N][NO] \\ k_3[N][O_2] \\ k_4[NO][O] \end{pmatrix}$$

Example: Zeldovich Mechanism of NO Formation, cont.

- To elucidate naturally conserved variables, use elementary row operations to cast system in non-unique row echelon form:

$$\frac{d}{dt} \begin{pmatrix} [N] \\ [NO] - [N] \\ 2[N_2] + [NO] + [N] \\ [O] + [N] \\ 2[O_2] + [NO] - [N] \end{pmatrix} = \begin{pmatrix} 1 & -1 & -1 & 1 \\ 0 & 0 & 2 & -2 \\ 0 & 0 & 0 & 0 \\ 0 & 0 & 0 & 0 \\ 0 & 0 & 0 & 0 \end{pmatrix} \begin{pmatrix} k_1[N_2][O] \\ k_2[N][NO] \\ k_3[N][O_2] \\ k_4[NO][O] \end{pmatrix}$$

- We are left with
 - two ODEs
 - three algebraic constraints: conservation of N atoms, O atoms, and number of molecules
 - easily reduced to two ODEs in two unknowns: $[N]$, $[NO]$.
- We will reduce the two ODEs to one ODE by imposing the manifold equation $\mathbf{W} \cdot \mathbf{F}(\mathbf{x}) = 0$, effectively equilibrating the fast time scale.

Example: Zeldovich Mechanism of NO Formation, cont.

- Consider first the intrinsic algebraic constraints:

$$\frac{d}{dt} \begin{pmatrix} 2[N_2] + [NO] + [N] \\ [O] + [N] \\ 2[O_2] + [NO] - [N] \end{pmatrix} = \begin{pmatrix} 0 \\ 0 \\ 0 \end{pmatrix}.$$

- Integrate these equations:

$$2[N_2] + [NO] + [N] = C_1,$$

$$[O] + [N] = C_2,$$

$$2[O_2] + [NO] - [N] = C_3.$$

The constants C_1, C_2, C_3 come from initial conditions.

- Solve equations for secondary variables in terms of $[N], [NO]$:

$$[N_2] = \frac{1}{2}(C_1 - [NO] - [N])$$

$$[O] = C_2 - [N]$$

$$[O_2] = \frac{1}{2}(C_3 - [NO] + [N])$$

- Note that rearrangement of the algebraic constraints demonstrates element and molecule conservation:

$$2[N_2] + [N] + [NO] = C_1,$$

$$2[O_2] + [NO] + [O] = C_2 + C_3,$$

$$[N] + [NO] + [N_2] + [O] + [O_2] = \frac{C_1 + C_3}{2} + C_2.$$

Example: Zeldovich Mechanism of NO Formation, cont.

- Substitution of algebraic constraints into ODEs for $[N]$ and $[NO]$ gives two autonomous ODEs well-suited for dynamic systems analysis:

$$\begin{aligned}\frac{d[N]}{dt} &= \frac{k_1}{2} (C_2 - [N]) (C_1 - [N] - [NO]) \\ &\quad - k_2 [N][NO] \\ &\quad - \frac{k_3}{2} [N] (C_3 + [N] - [NO]) \\ &\quad + k_4 [NO] (C_2 - [N]) \\ \frac{d[NO]}{dt} &= \frac{k_1}{2} (C_2 - [N]) (C_1 - [N] - [NO]) \\ &\quad - k_2 [N][NO] \\ &\quad + \frac{k_3}{2} [N] (C_3 + [N] - [NO]) \\ &\quad - k_4 [NO] (C_2 - [N])\end{aligned}$$

- Take as initial conditions

$$[N] = [NO] = [N_2] = [O] = [O_2] = 0.001 \frac{\text{mole}}{\text{cm}^3}.$$

- Equilibrium when right hand side zero
- Three roots-one physical, two unphysical:

$$\begin{pmatrix} [N] \\ [NO] \end{pmatrix} = \begin{pmatrix} 1.16 \times 10^{-11} \frac{\text{mole}}{\text{cm}^3} \\ 2.78 \times 10^{-6} \frac{\text{mole}}{\text{cm}^3} \end{pmatrix}, \begin{pmatrix} -1.15 \times 10^{-11} \frac{\text{mole}}{\text{cm}^3} \\ -2.78 \times 10^{-6} \frac{\text{mole}}{\text{cm}^3} \end{pmatrix}, \begin{pmatrix} -2.00 \times 10^{-3} \frac{\text{mole}}{\text{cm}^3} \\ 0.00 \times 10^0 \frac{\text{mole}}{\text{cm}^3} \end{pmatrix},$$

Example: Zeldovich Mechanism of NO Formation, cont.

- Linearization of equations near physical equilibrium gives

$$\frac{d}{dt} \begin{pmatrix} [N] - 1.16 \times 10^{-11} \\ [NO] - 2.78 \times 10^{-6} \end{pmatrix} = \begin{pmatrix} -9.67 \times 10^8 & 3.38 \times 10^3 \\ 8.11 \times 10^8 & -4.03 \times 10^3 \end{pmatrix} \mathbf{F}_x$$

$$\frac{d}{dt} \begin{pmatrix} [N] - 1.16 \times 10^{-11} \\ [NO] - 2.78 \times 10^{-6} \end{pmatrix} = \begin{pmatrix} -0.766 & -0.643 \\ 0.643 & -0.766 \end{pmatrix} \mathbf{Q}$$

$$\begin{pmatrix} -9.67 \times 10^8 & 3.38 \times 10^3 \\ 0 & -1.19 \times 10^3 \end{pmatrix} \mathbf{U}$$

$$\begin{pmatrix} -0.766 & 0.643 \\ -0.643 & -0.766 \end{pmatrix} \mathbf{Q}^T$$

$$\begin{pmatrix} [N] - 1.16 \times 10^{-11} \\ [NO] - 2.78 \times 10^{-6} \end{pmatrix}$$

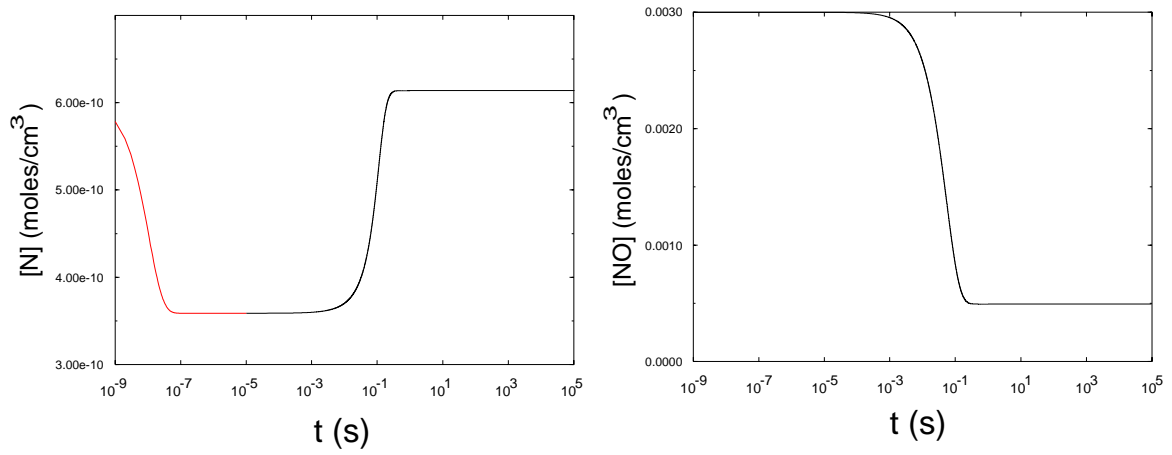
- Condition number (stiffness ratio) = $\left| \frac{-9.67 \times 10^8}{-1.19 \times 10^3} \right| = 8.1 \times 10^5$.
- Locally the ILDM is defined by

$$\mathbf{W} \cdot \mathbf{F}(\mathbf{x}) = 0,$$

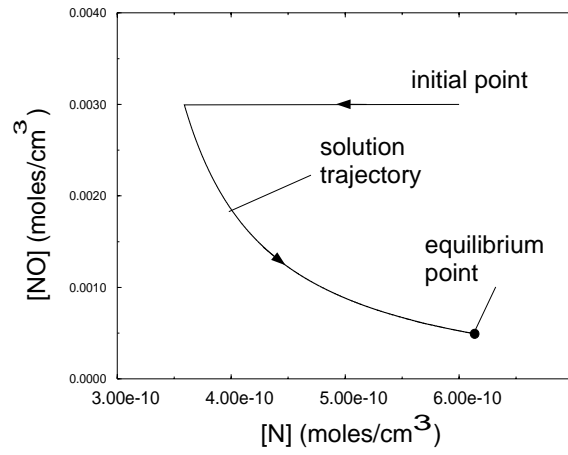
$$\begin{pmatrix} -0.766 & 0.643 \end{pmatrix} \begin{pmatrix} F_1([N], [NO]) \\ F_2([N], [NO]) \end{pmatrix} = 0.$$

- Use arc length continuation methods to define complete ILDM
- The physical equilibrium has negative eigenvalues: stable.
- The non-physical equilibria have positive eigenvalues: unstable.

Time Variation of [N] and [NO] Concentration

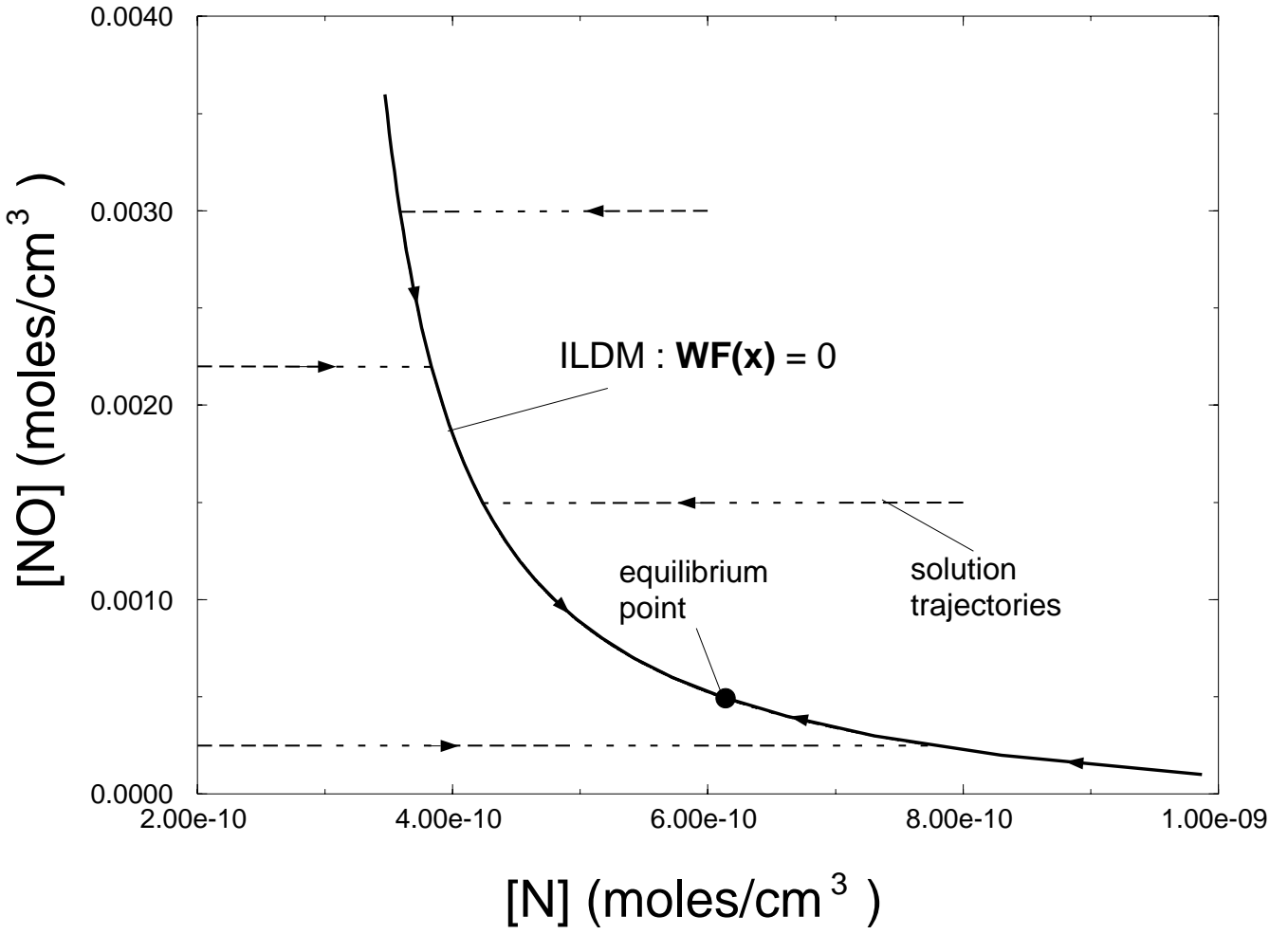


[N] - [NO] Phase Plane



Condition Number is of the order of 1e+6

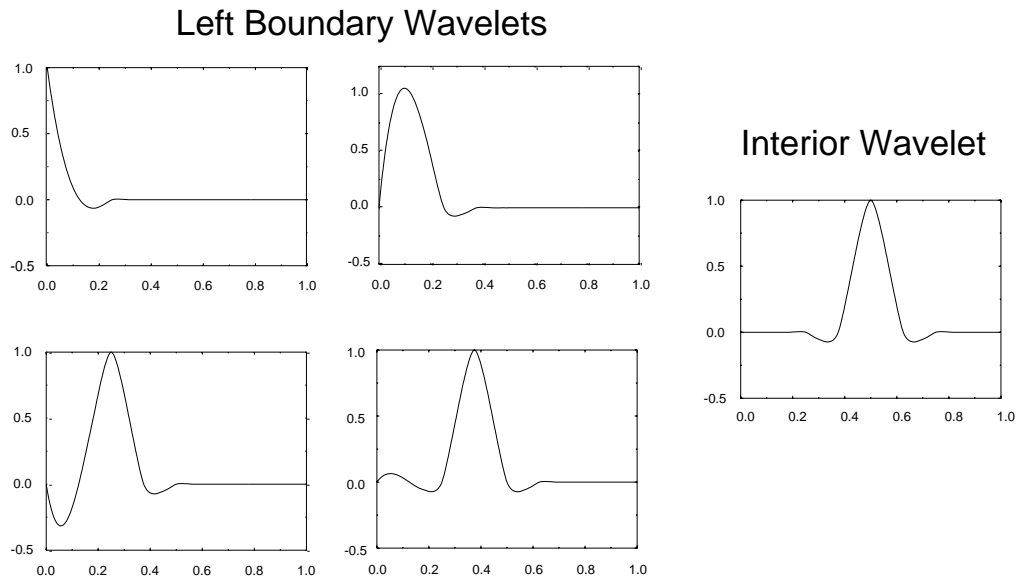
[N] - [NO] Phase Plane



Adaptive Multilevel Wavelet Collocation Technique

- Summary of standard spatial discretization techniques
 - Finite difference-good spatial localization, poor spectral localization, and slow convergence,
 - Finite element- good spatial localization, poor spectral localization, and slow convergence,
 - Spectral-good spectral localization, poor spatial localization, but fast convergence.
- Wavelet technique
 - See e.g. Vasilyev and Paolucci, “A Fast Adaptive Wavelet Collocation Algorithm for Multidimensional PDEs,” *J. Comp. Phys.*, 1997,
 - Basis functions have compact support,
 - Well-suited for problems with widely disparate spatial scales,
 - Good spatial and spectral localization, and fast (spectral) convergence,
 - Easy adaptable to steep gradients via adding collocation points,
 - Spatial adaptation is automatic and dynamic to achieve prescribed error tolerance.

Wavelet Basis Functions



- Boundary-modified Daubechies autocorrelation functions and interior Daubechies autocorrelation function of order four
- Scaling function

$$\phi_{j,k}(x) = \phi(2^j x - k)$$

- Definition of the wavelet function on the first level

$$\psi_{1,0}(x) = \phi(2x - 1)$$

- Definition of the wavelet function on j level

$$\psi_{j,k+1}(x) = \psi(2^{j-1}x - k)$$

Algorithm Description

- Approximate initial function using wavelet basis,

$$\mathbf{P}^J u(x) = \sum_k u_{0,k} \phi_{0,k}(x) + \sum_{j=1}^J \sum_k d_{j,k} \psi_{j,k}(x)$$

- Discard non-essential wavelets if amplitude below threshold value (here we look only at P , T , u , and ρ , species could be included),

$$\mathbf{P}^J u(x) = u_{\geq}^J(x) + u_{<}^J(x)$$

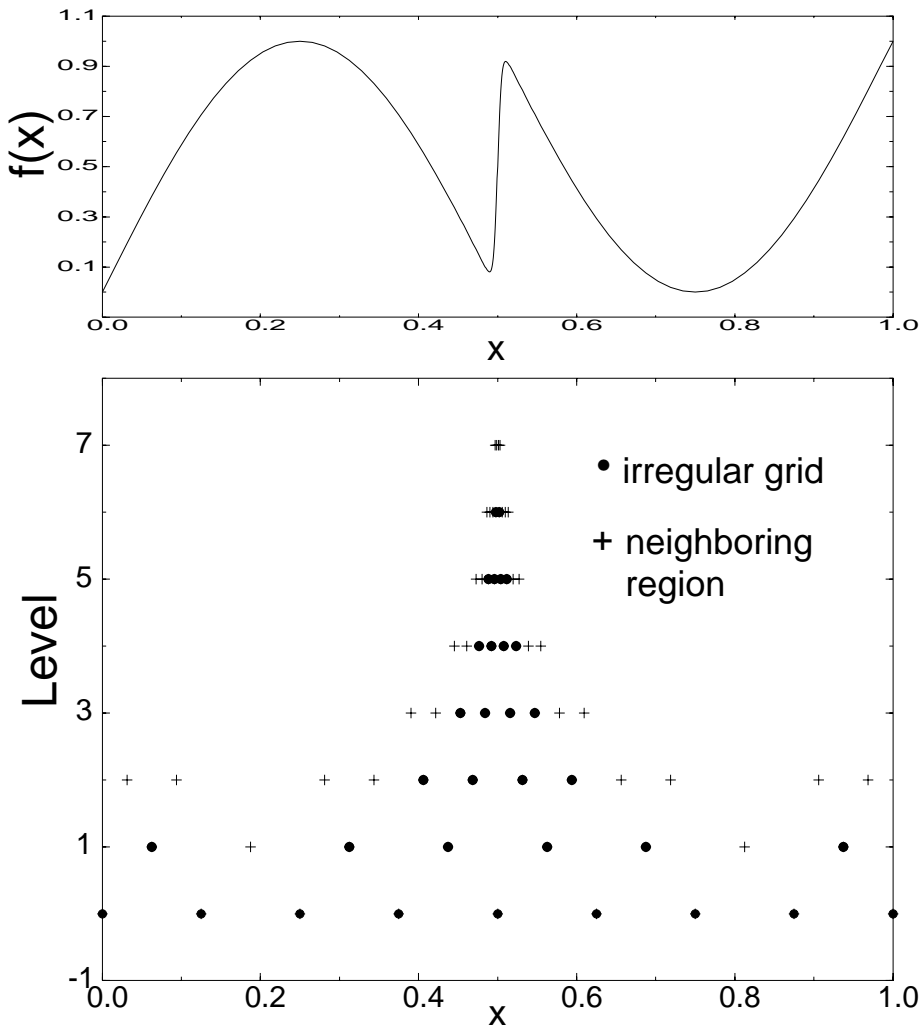
$$u_{\geq}^J(x) = \sum_k u_{0,k} \phi_{0,k}(x) + \sum_{j=1}^J \sum_k d_{j,k} \psi_{j,k}(x), |d_{j,k}| \geq \epsilon$$

$$u_{<}^J(x) = \sum_{j=1}^J \sum_k d_{j,k} \psi_{j,k}(x), |d_{j,k}| < \epsilon$$

- Assign a collocation point to every essential wavelet,
- Establish a neighboring region of potentially essential wavelets,
- Discretize the spatial derivatives; five points used here (related to order of wavelet family),
- Integrate in time; linearized trapezoidal method (implicit) used here,
- Repeat

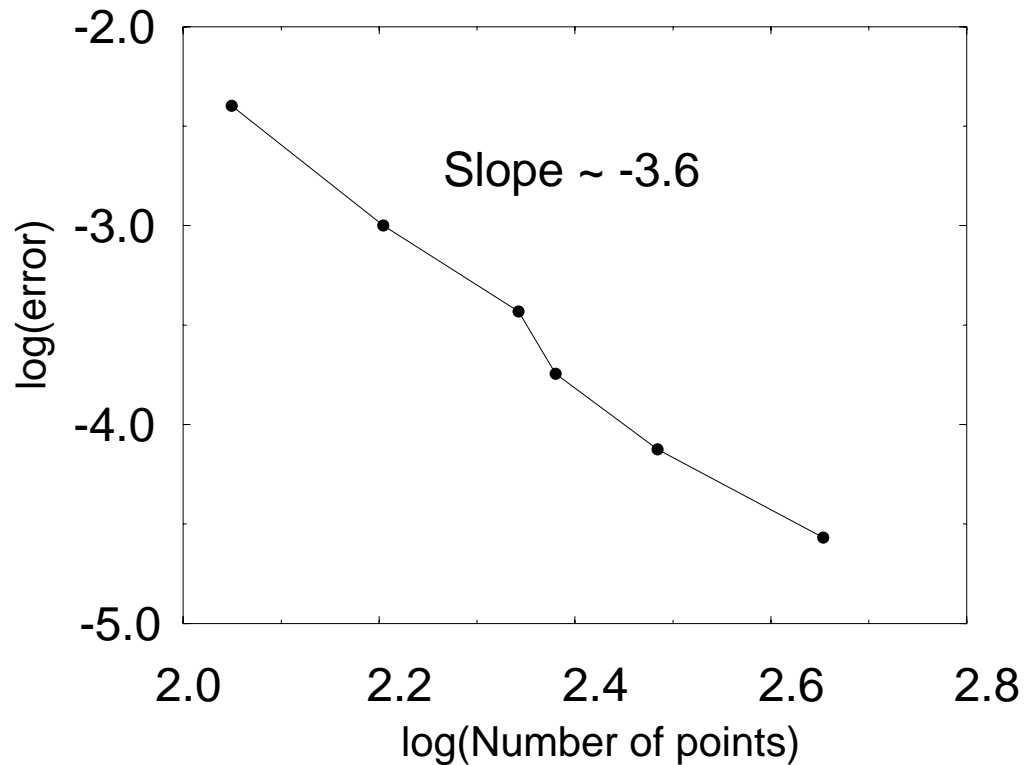
Sample Wavelet Approximation to Arbitrary Function

Arbitrary Function with Variation on Long and Short Scales



- Function shown has large and small length scale variation,
- Wavelets concentrated in regions of steep gradients.

Sample Calculation Demonstrating Rapid Convergence



$$\frac{\partial u}{\partial t} - \frac{\partial u}{\partial x} = 0, \quad x \in [0, 1], \quad t \in [0, 0.2]$$

$$u(x, 0) = g(x), \quad u(1, t) = g(t)$$

$$g(s) = \sin(2\pi s) + \exp\left(-10000(s - 1/2)^2\right)$$

- exact solution available,
- L_∞ norm used for error calculation,
- Convergence rate ($N^{3.6}$) roughly consistent with wavelet order (4).

Ignition Delay in Premixed H_2 - O_2

- Consider standard problem of Fedkiw, Merriman, and Osher, *J. Comp. Phys.*, 1996,
- Shock tube with premixed H_2 , O_2 , and Ar in 2/1/7 molar ratio,
- Initial inert shock propagating in tube,
- Reaction commences shortly after reflection off end wall,
- Detonation soon develops,
- Model assumptions
 - One-dimensional,
 - No diffusion (one case); mass, momentum, and energy diffusion (another case),
 - Nine species, thirty-seven reactions,
 - Ideal gases with variable specific heats.

Compressible Reactive Navier-Stokes Equations for H_2-O_2 Problem

$$\frac{\partial \rho}{\partial t} + \frac{\partial}{\partial x} (\rho u) = 0, \quad \text{mass}$$

$$\frac{\partial}{\partial t} (\rho u) + \frac{\partial}{\partial x} (\rho u^2 + P - \tau) = 0, \quad \text{momentum}$$

$$\frac{\partial}{\partial t} \left(\rho \left(e + \frac{u^2}{2} \right) \right) + \frac{\partial}{\partial x} \left(\rho u \left(e + \frac{u^2}{2} \right) + u(P - \tau) + q \right) = 0, \quad \text{energy}$$

$$\frac{\partial}{\partial t} (\rho Y_i) + \frac{\partial}{\partial x} (\rho u Y_i + j_i) = \sum_{j=1}^M a_j T^{\alpha_j} \exp \left(\frac{-E_j}{\mathfrak{R}T} \right) \nu_{ij} M_i \prod_{k=1}^N \left(\frac{\rho Y_k}{M_k} \right)^{\nu_{kj}}, \quad \text{species}$$

$$P = \rho \mathfrak{R}T \sum_{i=1}^N \frac{Y_i}{M_i}, \quad \text{thermal equation of state}$$

$$e = \sum_{i=1}^N Y_i \left(h_i^o + \int_{T_o}^T c_{pi}(\hat{T}) d\hat{T} \right) - \frac{P}{\rho}, \quad \text{caloric equation of state}$$

$$\tau = \frac{4}{3} \mu \frac{\partial u}{\partial x}, \quad \text{Newtonian gas with Stokes' assumption}$$

$$j_i = -\rho \sum_{j=1}^N \mathcal{D}_{ij} \frac{\partial Y_j}{\partial x}, \quad \text{Fick's law}$$

$$q = -k \frac{\partial T}{\partial x} + \sum_{i=1}^N j_i \left(h_i^o + \int_{T_o}^T c_{pi}(\hat{T}) d\hat{T} \right) \quad \text{augmented Fourier's law.}$$

$N = 9$ species: $H_2, O_2, H, O, OH, H_2O_2, H_2O, HO_2, Ar$

$M = 37$ reactions

Operator Splitting Technique

- Equations are of form

$$\frac{\partial}{\partial t} \mathbf{q}(x, t) + \frac{\partial}{\partial x} \mathbf{f}(\mathbf{q}(x, t)) = \mathbf{g}(\mathbf{q}(x, t)).$$

where

$$\mathbf{q} = \left(\rho, \rho u, \rho \left(e + \frac{u^2}{2} \right), \rho Y_i \right)^T$$

- \mathbf{f} models convection and diffusion
- \mathbf{g} models reaction source terms
- Splitting
 1. Inert convection diffusion step:

$$\begin{aligned} \frac{\partial}{\partial t} \mathbf{q}(x, t) + \frac{\partial}{\partial x} \mathbf{f}(\mathbf{q}(x, t)) &= 0, \\ \frac{d}{dt} \mathbf{q}_i(t) &= -\Delta_x \mathbf{f}(\mathbf{q}_i(t)). \end{aligned}$$

Δ_x is either Godunov *or* wavelet discretization operator.

2. Reaction source term step:

$$\begin{aligned} \frac{\partial}{\partial t} \mathbf{q}(x, t) &= \mathbf{g}(\mathbf{q}(x, t)), \\ \frac{d}{dt} \mathbf{q}_i(t) &= \mathbf{g}(\mathbf{q}_i(t)). \end{aligned}$$

- Operator splitting with implicit stiff source solution can induce non-physical wave speeds! (LeVeque and Yee, *JCP* 1990)

ILDDM Implementation in Operator Splitting

- Form of equations in source term step:

$$\frac{d}{dt} \begin{pmatrix} \rho \\ \rho u \\ \rho \left(e + \frac{u^2}{2} \right) \\ \rho Y_i \end{pmatrix} = \begin{pmatrix} 0 \\ 0 \\ 0 \\ \omega \end{pmatrix}.$$

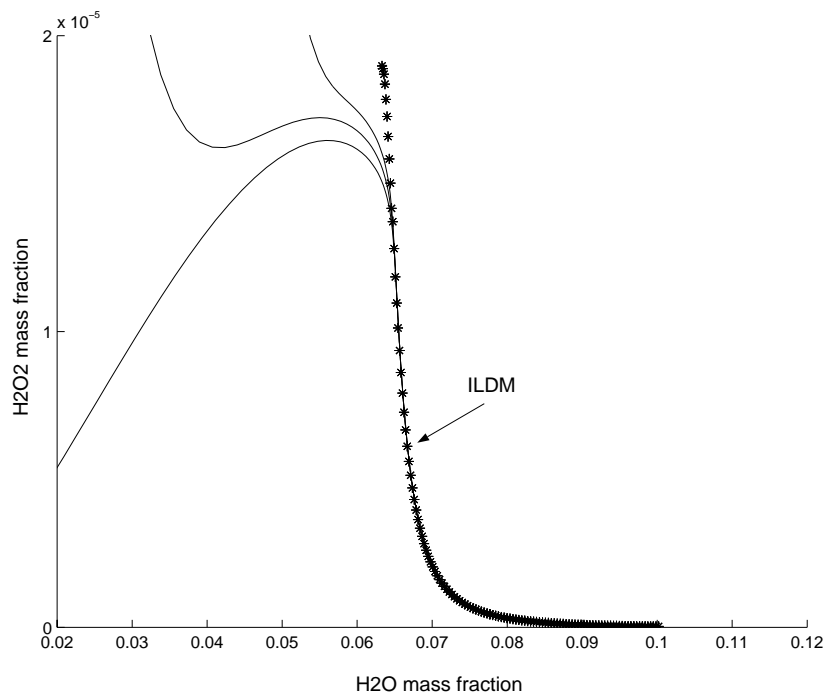
- Equations reduce to

$$\rho = \rho_o, \quad u = u_o, \quad e = e_o,$$
$$\frac{dY_i}{dt} = \frac{\omega}{\rho_o}.$$

- ω has dependency on ρ , e , and Y_i
- ODEs for Y_i can be attacked with manifold methods when manifold with ρ , e , H and O parameterization is available.
- In premixed problem, H and O element concentrations are remarkably constant, reducing the dimension by two!
- Full equations integrated until sufficiently close to manifold
- Once on manifold, simple projection used to return to manifold following convection-diffusion step

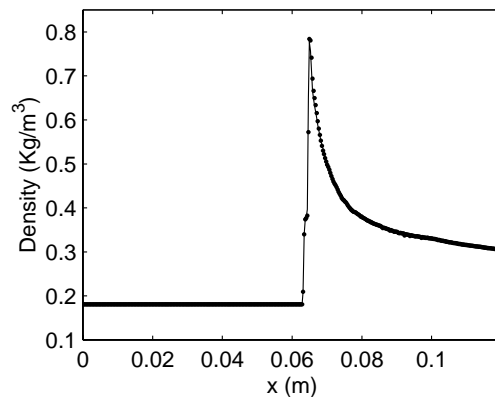
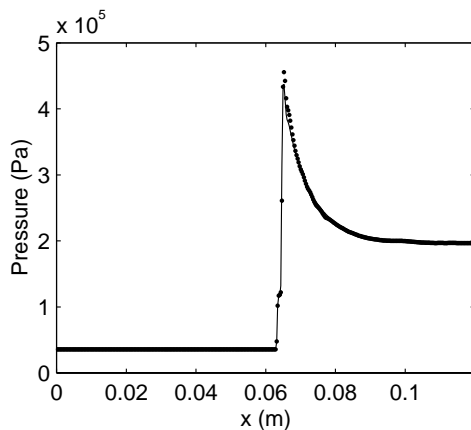
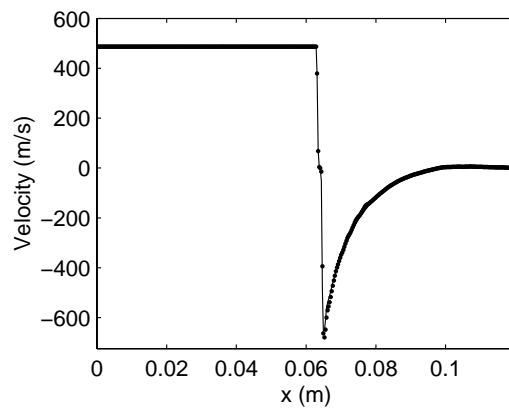
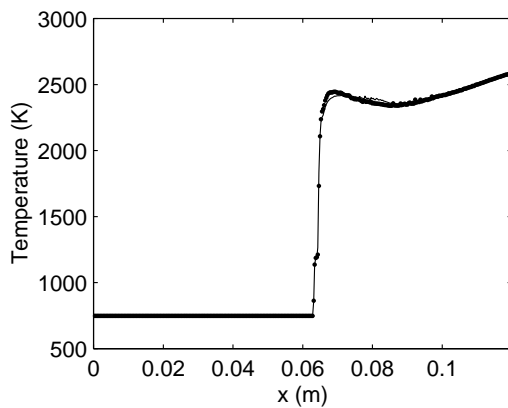
Sample ILDM for $H_2 - O_2$

- Projection of ILDM in H_2O , H_2O_2 plane,
- Adiabatic ($e = 525 \text{ kJ/kg}$), isochoric ($\rho = 0.25 \text{ kg/m}^3$), element concentrations of H and O constant,
- Complete manifold tabulated in three dimensions: ρ, e, Y_{H_2O} ,
- So we have e.g. $P(\rho, e, Y_{H_2O}), T(\rho, e, Y_{H_2O}), Y_H(\rho, e, Y_{H_2O}), \dots$
- Linear interpolation used for points not in table,
- Captures $\sim 0.1 \mu s$ reaction events.

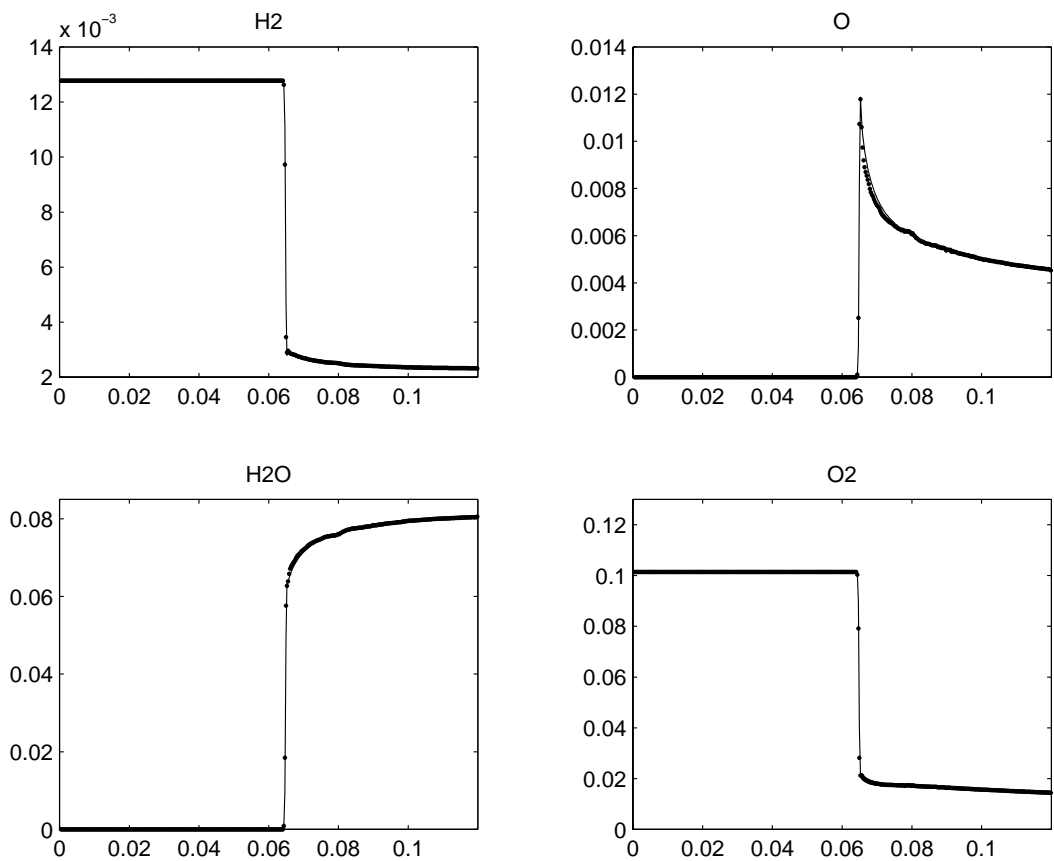


Inviscid $H_2 - O_2$ Ignition Delay with and without ILDM

- No diffusion,
- Godunov spatial discretization, 400 uniform finite difference cells,
- Implicit (trapezoidal) convection step; Implicit (dlsode) *or* ILDM reaction step,
- Correction of Fedkiw adopted to suppress artificial entropy layer after shock reflection (see Menikoff, 1994).

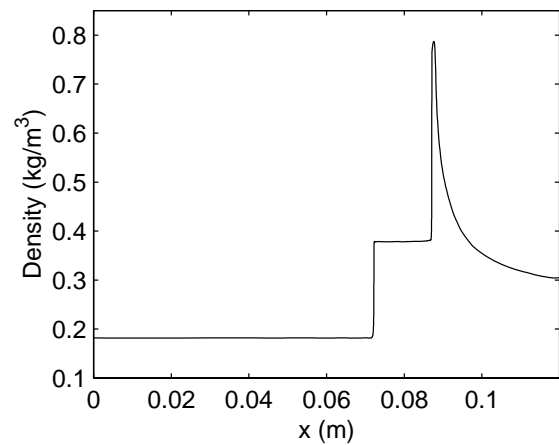
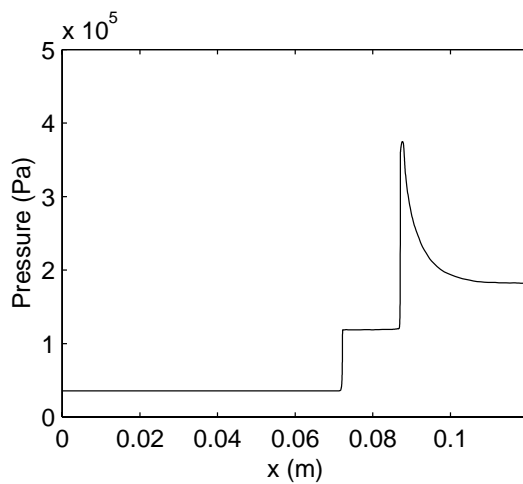
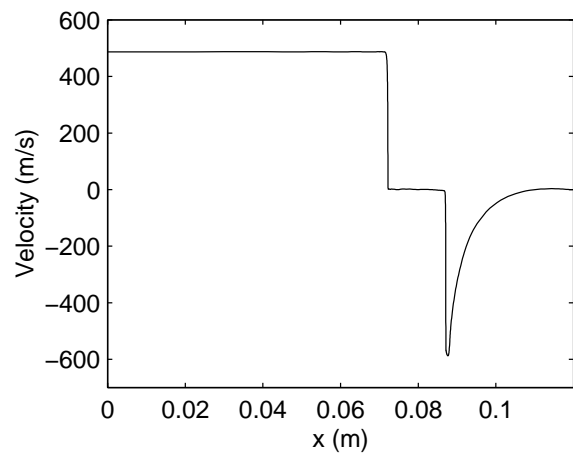
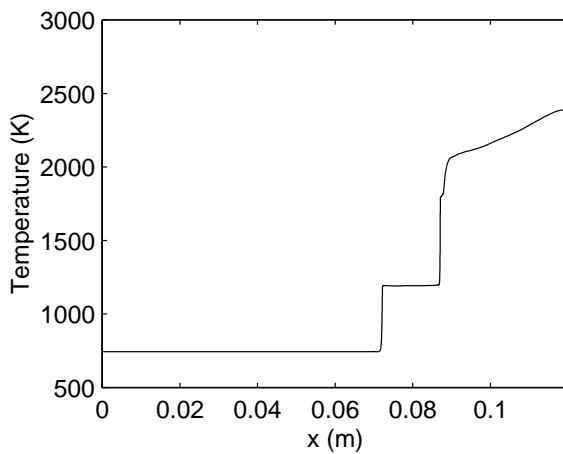


Inviscid $H_2 - O_2$ Ignition Delay with and without ILDM



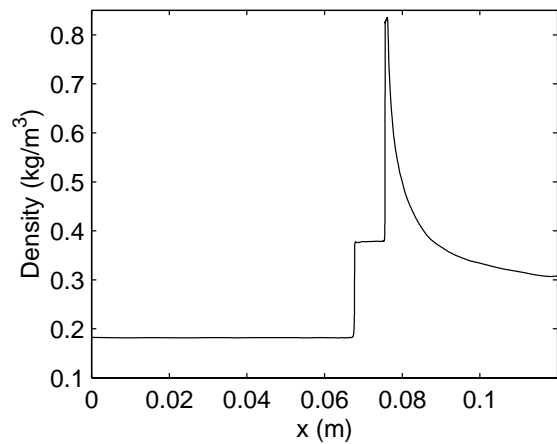
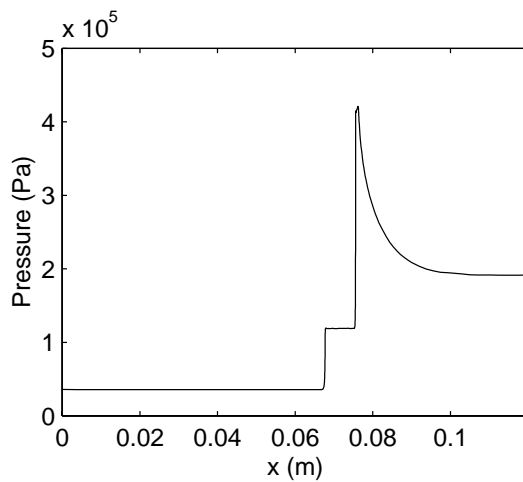
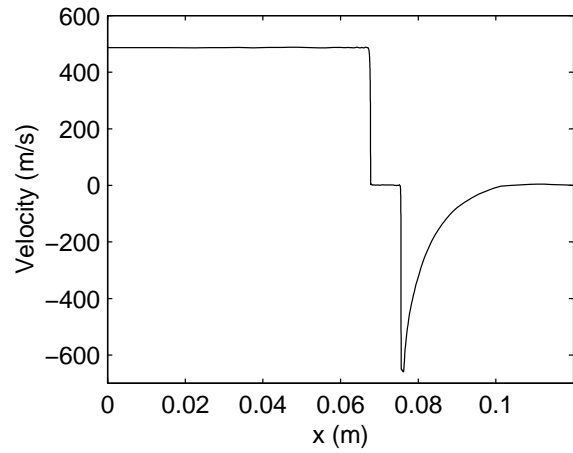
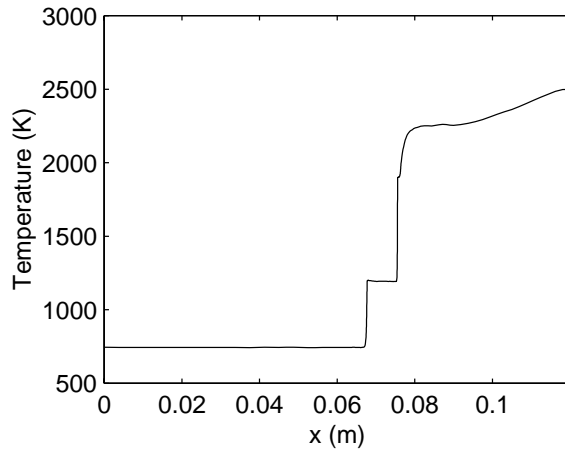
Viscous $H_2 - O_2$ Ignition Delay with Wavelets

- Mass, momentum, and energy diffusion modelled,
- Wavelet spatial discretization, explicit convection-diffusion time stepping, implicit reaction time stepping,
- 300 collocation points, 15 wavelet levels,
- *Viscous shocks, induction zones, and entropy layers spatially resolved!*
- $t = 180 \mu s$.



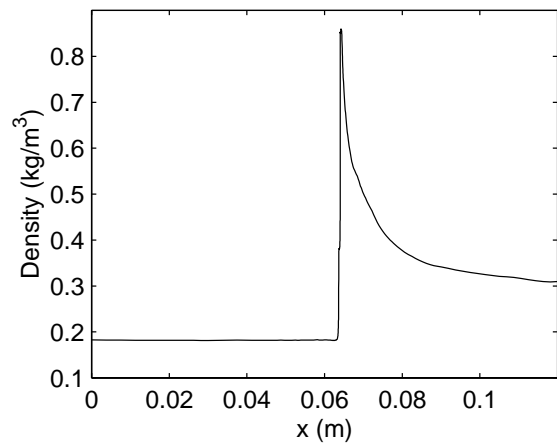
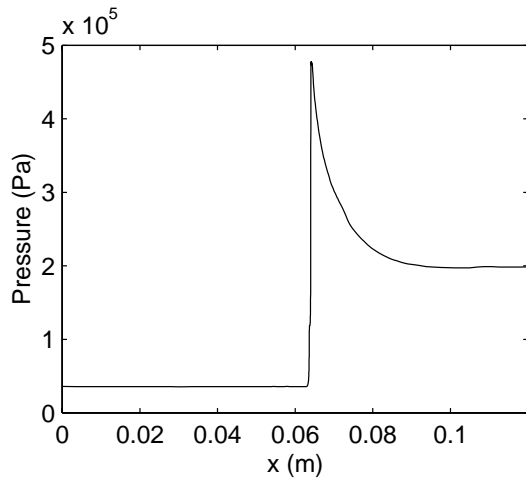
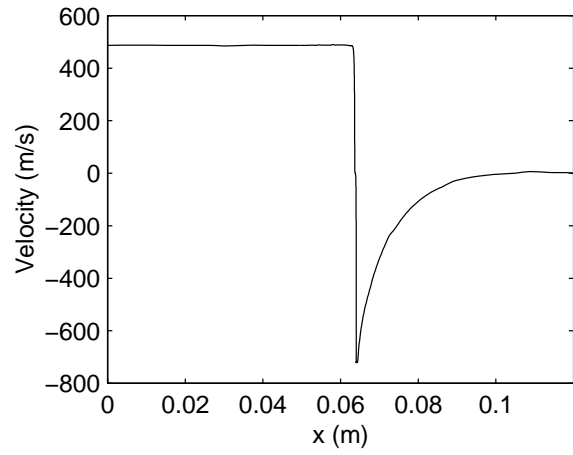
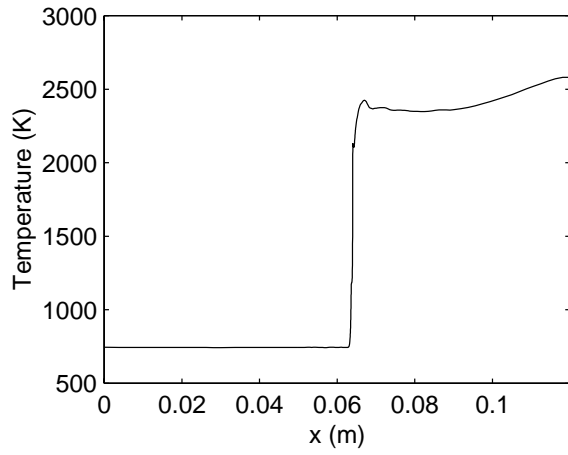
Viscous $H_2 - O_2$ Ignition Delay with Wavelets

• $t = 190 \mu s$



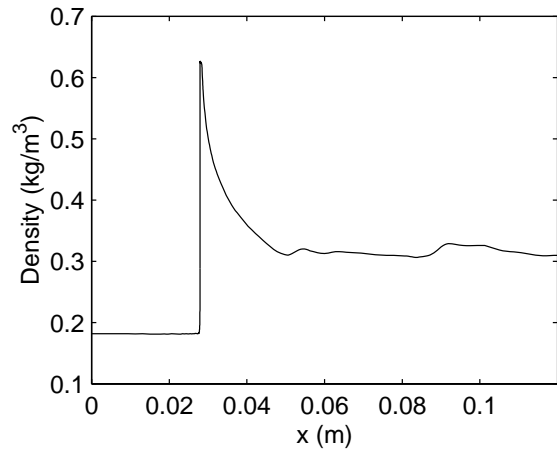
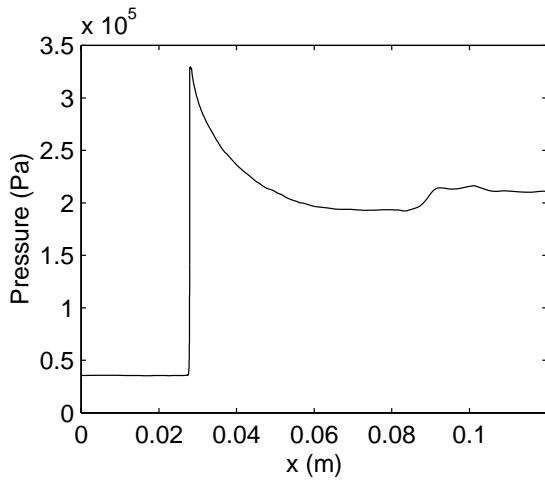
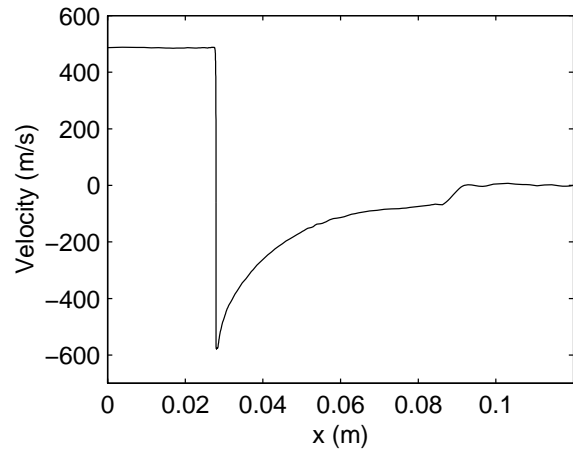
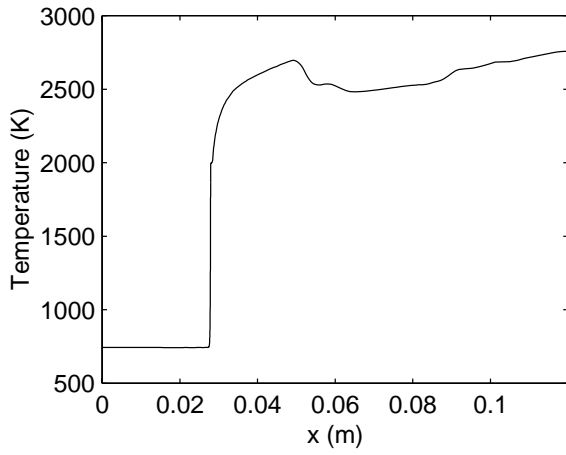
Viscous $H_2 - O_2$ Ignition Delay with Wavelets

- $t = 200 \mu s$



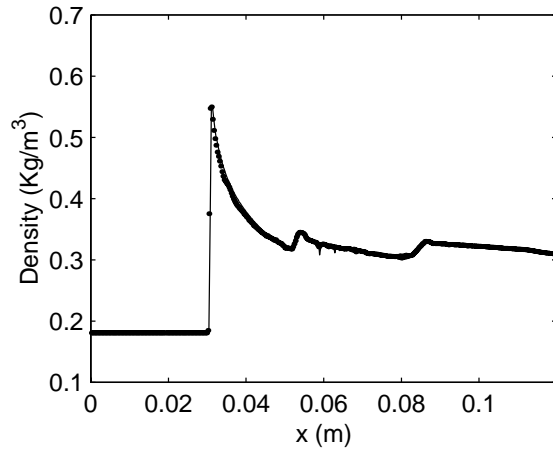
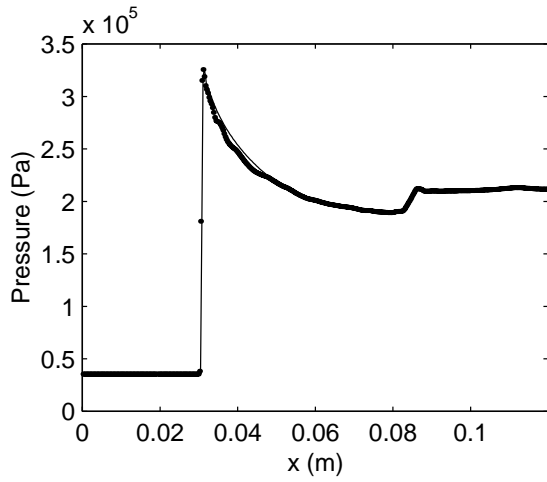
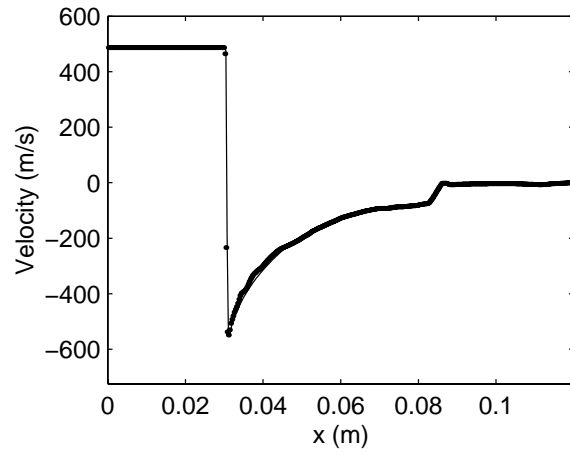
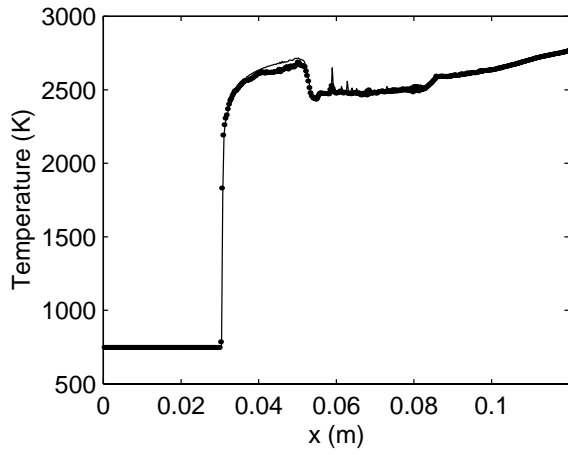
Viscous $H_2 - O_2$ Ignition Delay with Wavelets

• $t = 230 \mu s$



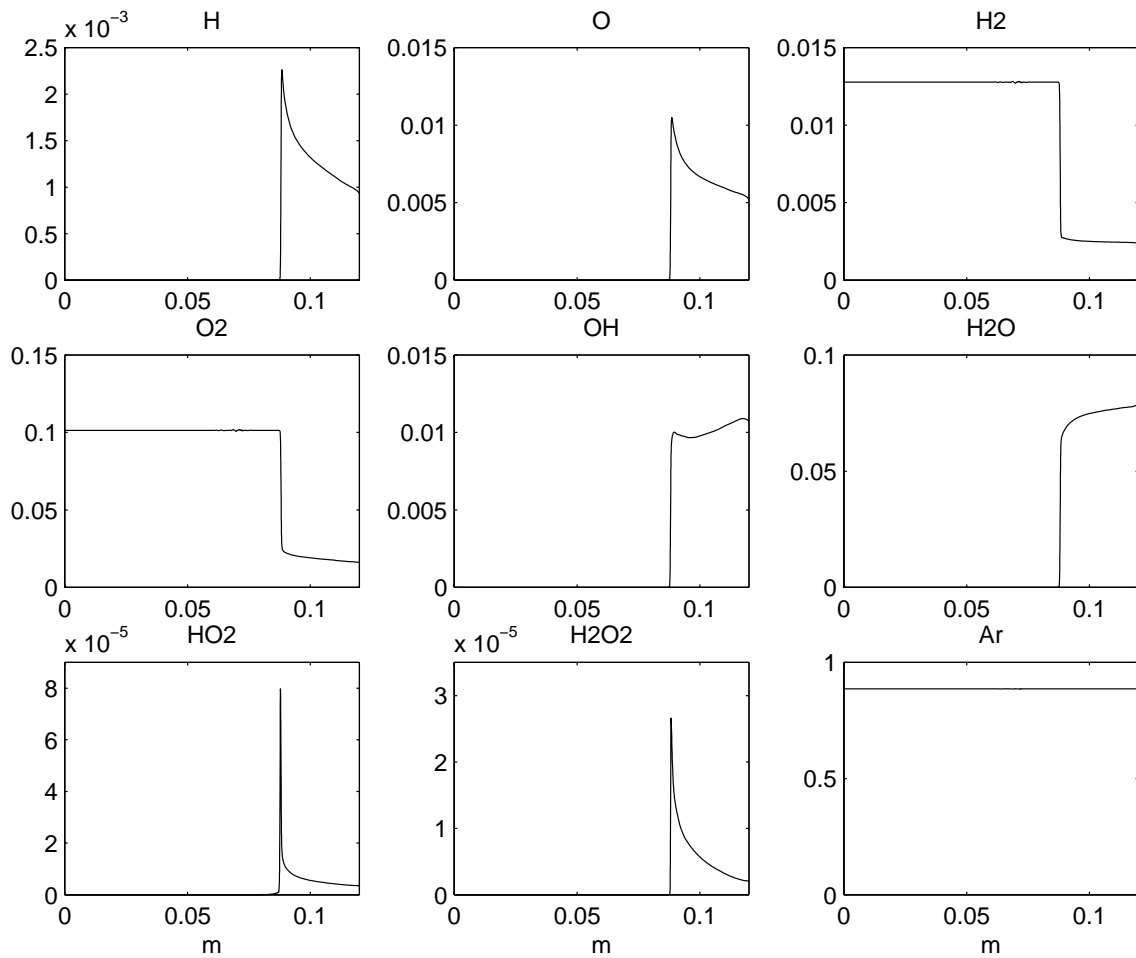
Comparison with Inviscid/ILDM Result at Same Time

• $t = 230 \mu s$



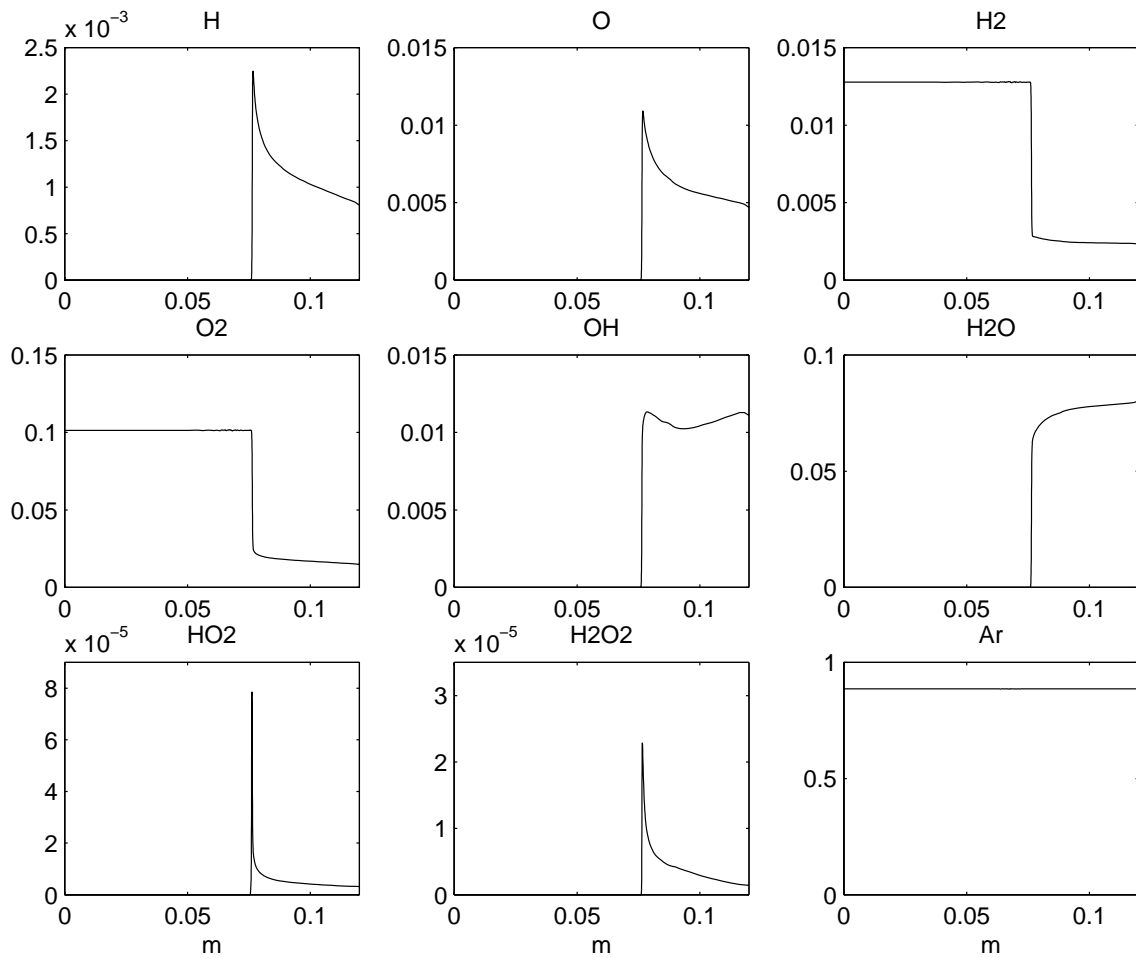
Viscous $H_2 - O_2$ Ignition Delay with Wavelets

- $t = 180 \mu s$
- species mass fractions plotted vs. distance



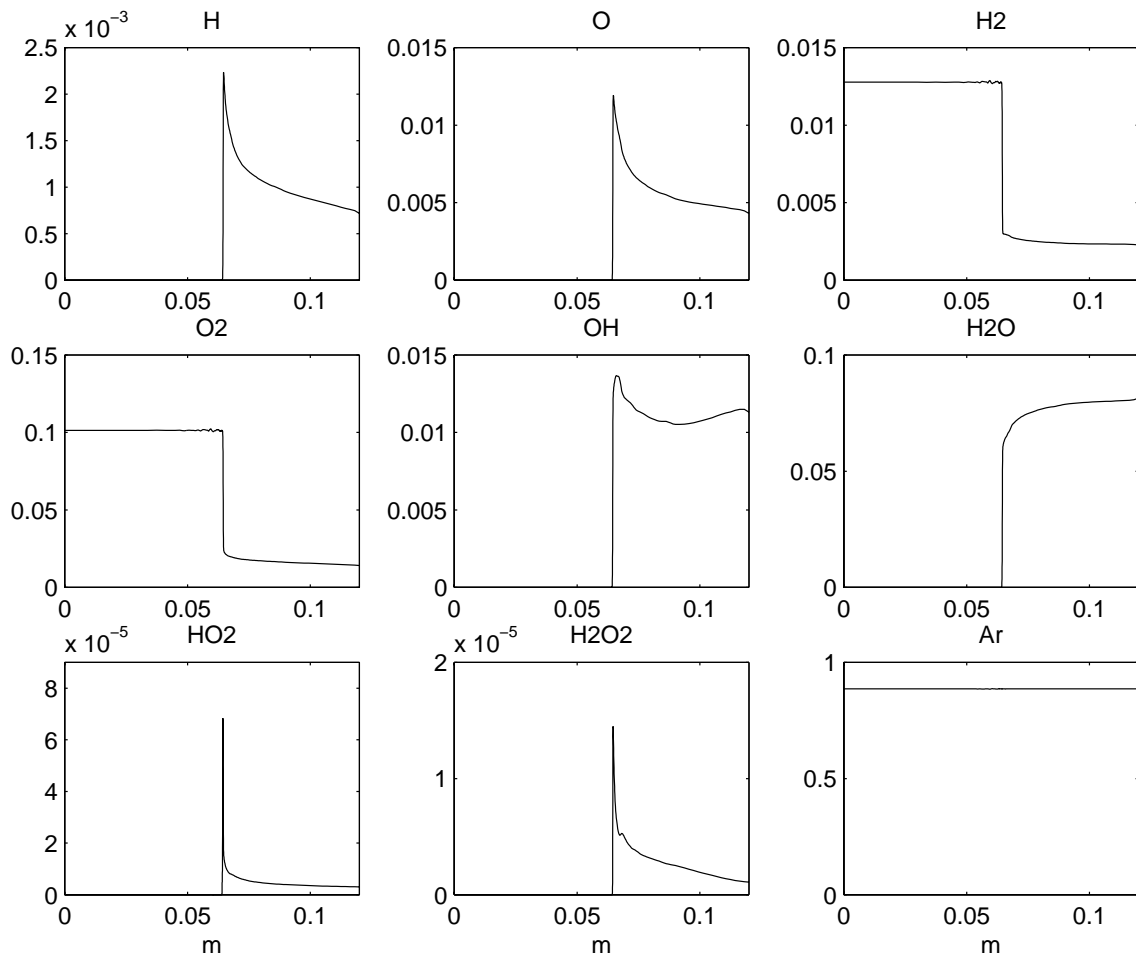
Viscous $H_2 - O_2$ Ignition Delay with Wavelets

- $t = 190 \mu s$
- species mass fractions plotted vs. distance



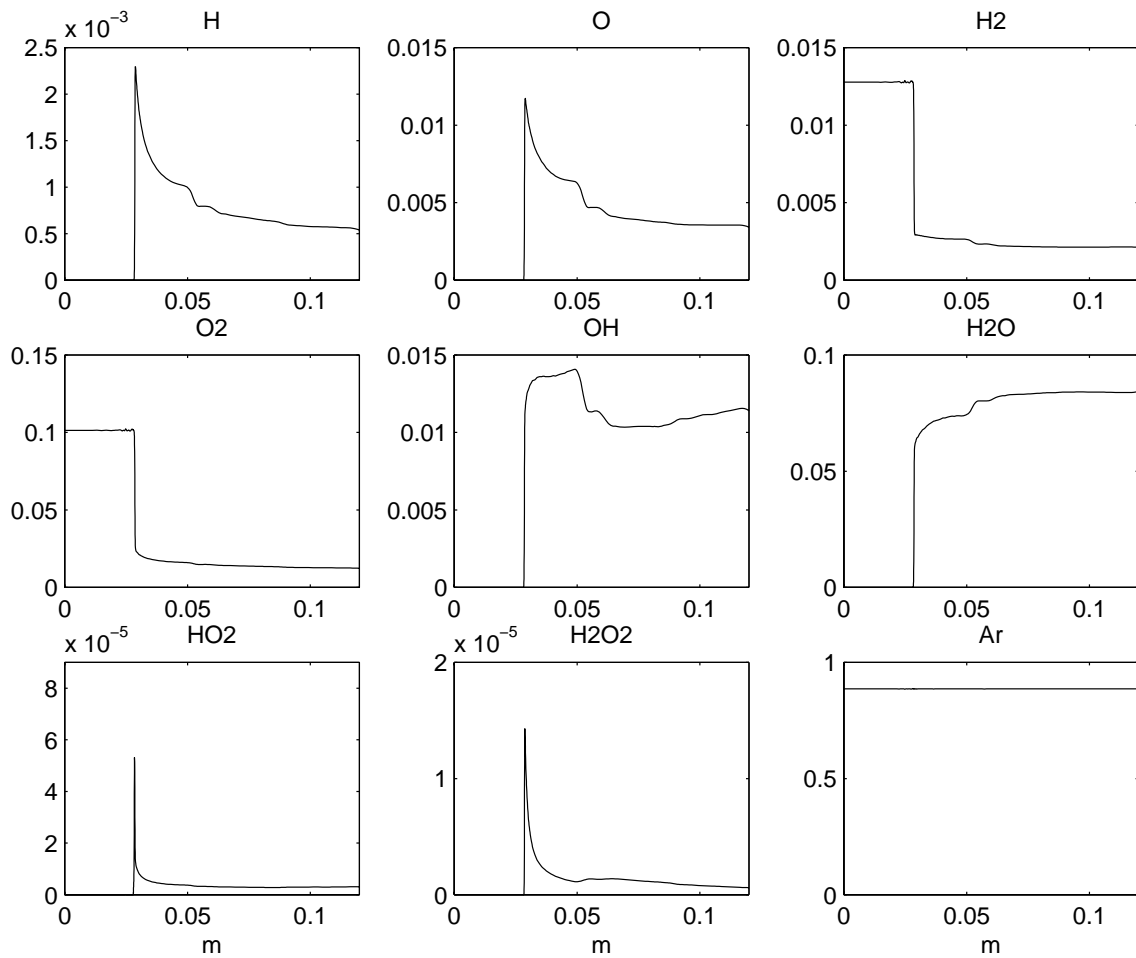
Viscous $H_2 - O_2$ Ignition Delay with Wavelets

- $t = 200 \mu s$
- species mass fractions plotted vs. distance



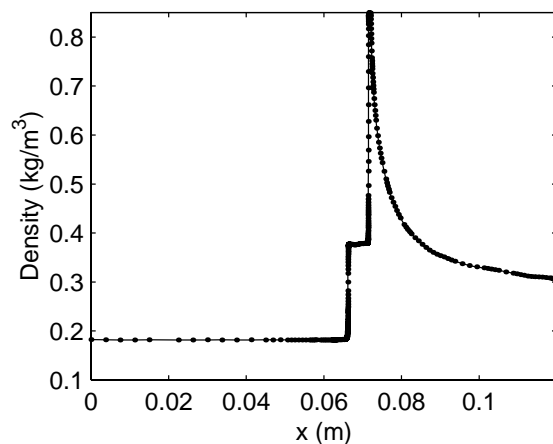
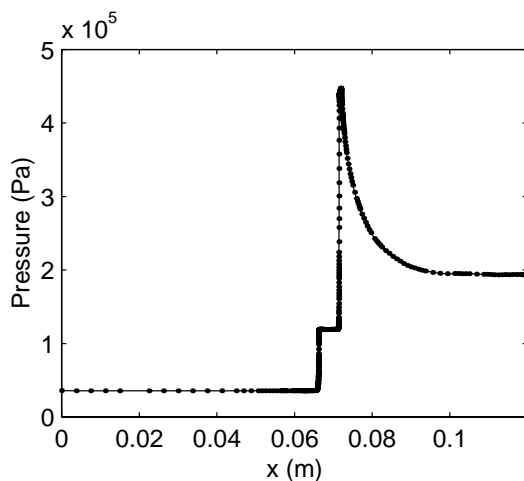
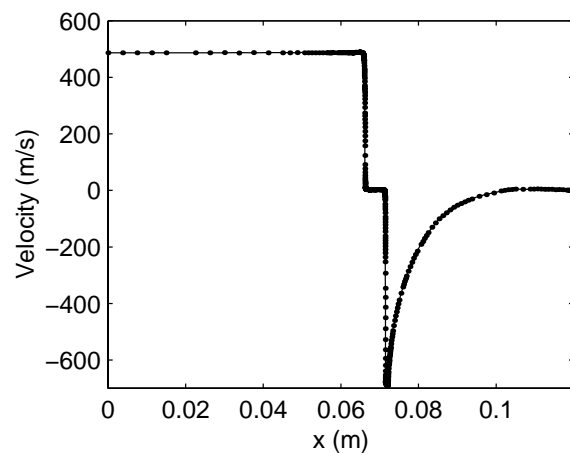
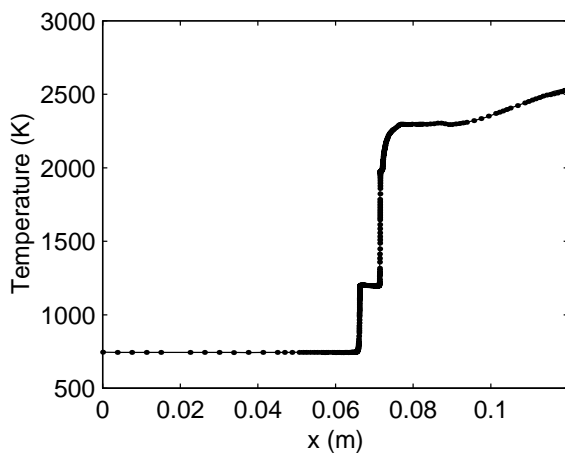
Viscous $H_2 - O_2$ Ignition Delay with Wavelets

- $t = 230 \mu s$
- species mass fractions plotted vs. distance



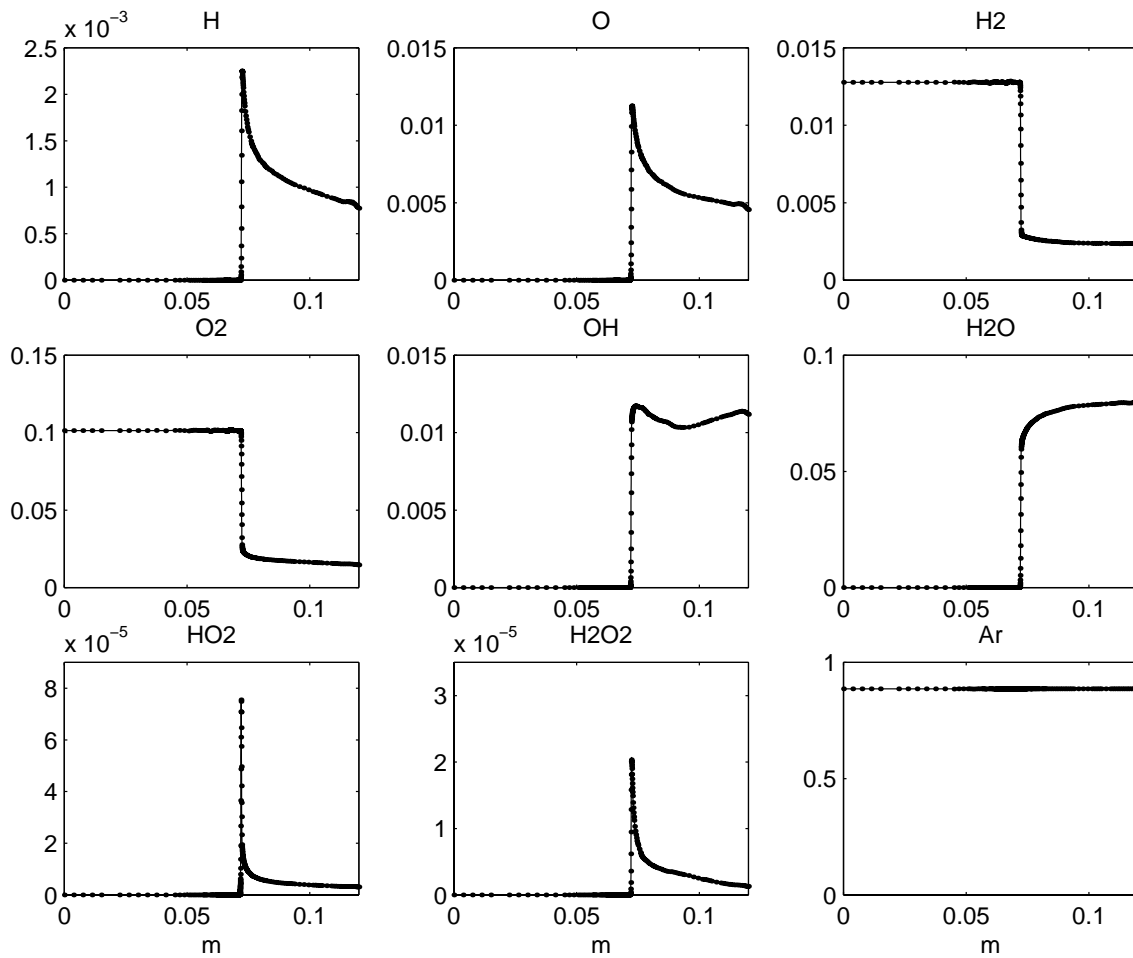
Viscous $H_2 - O_2$ Ignition Delay with Wavelets and ILDM

- $t = 195 \mu s$
- ILDM gives nearly identical results as full chemistry
- computational time ~ 10 hours on 330 MHz Sun Ultra10 for full chemistry and ILDM !?
- ILDM *will improve dramatically* when inefficient I/O is eliminated (factor of at least 10 for simpler problems)



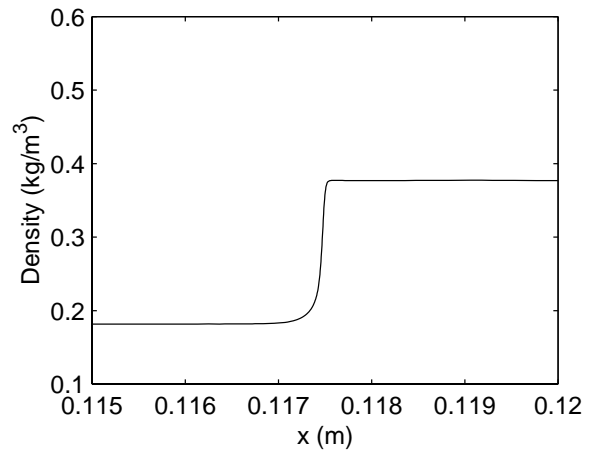
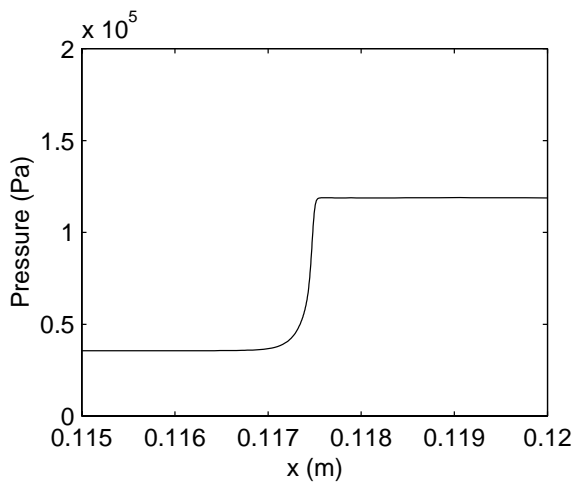
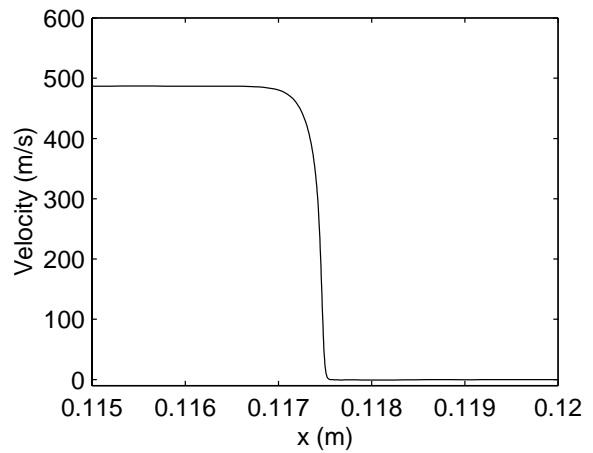
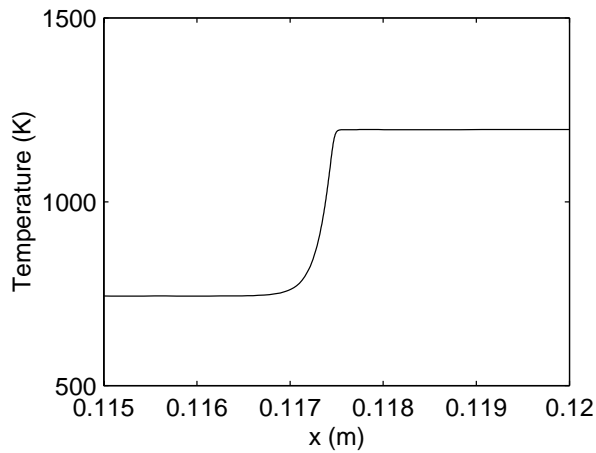
Viscous $H_2 - O_2$ Ignition Delay with Wavelets and ILDM

- $t = 195 \mu s$
- ILDM gives nearly identical results as full chemistry



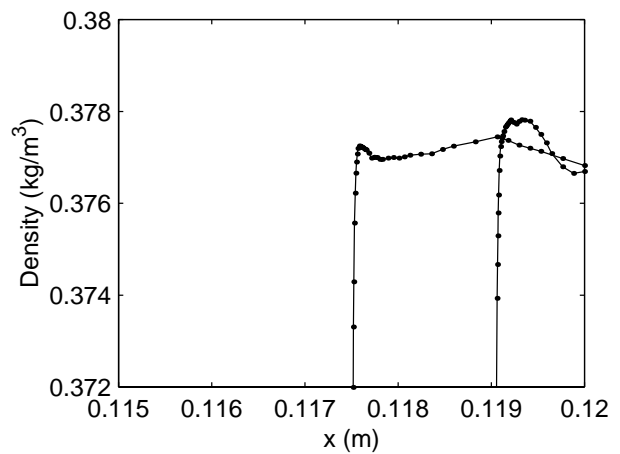
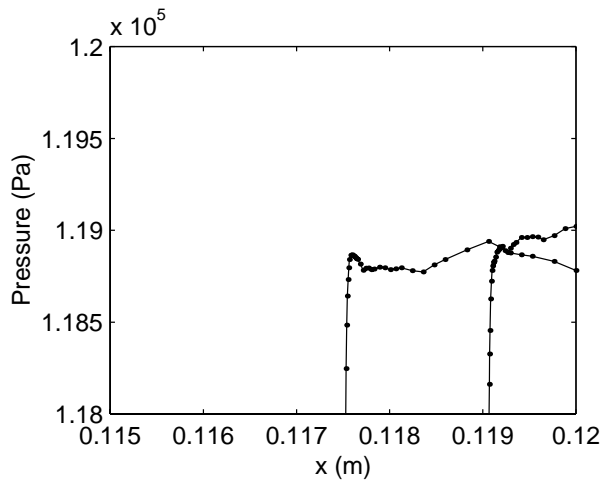
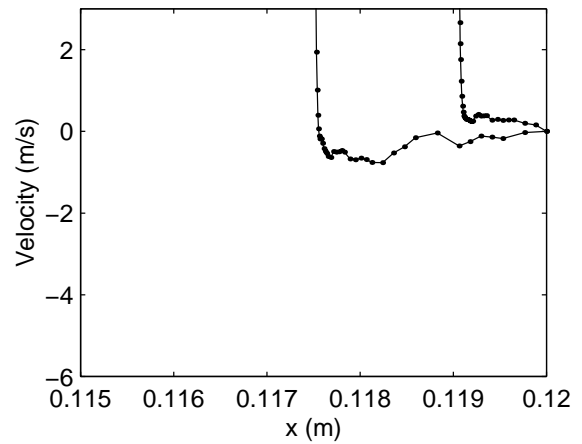
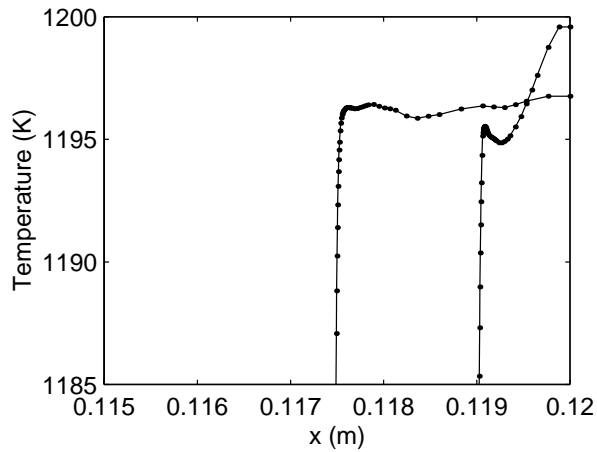
Post Reflection Entropy Layer?: Viscous Wavelet Results

- No significant entropy layer evident on macroscale after shock reflection when resolved viscous terms considered,
- Inviscid codes with coarse gridding introduce a larger entropy layer due to numerical diffusion,
- Unless suppressed, unphysically accelerates reaction rate.



Post Reflection Entropy Layer: Viscous Wavelet Results

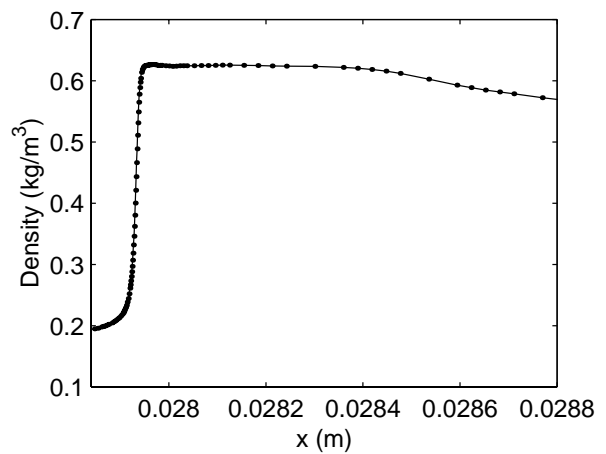
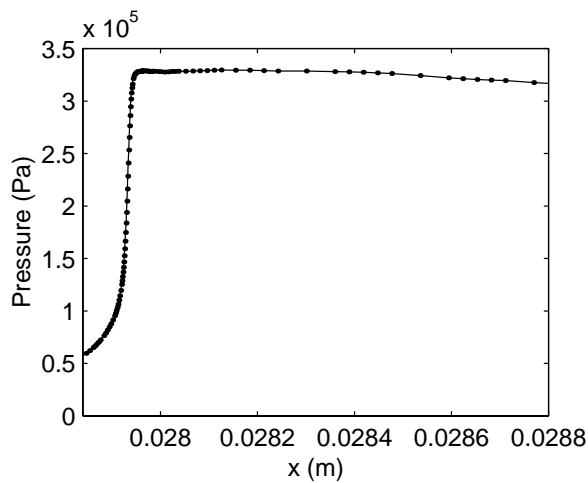
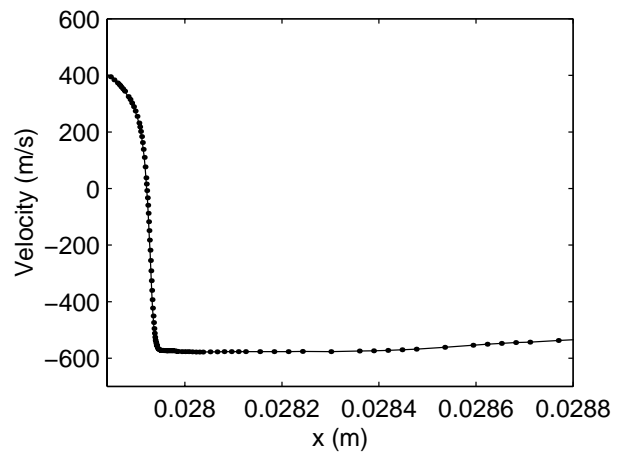
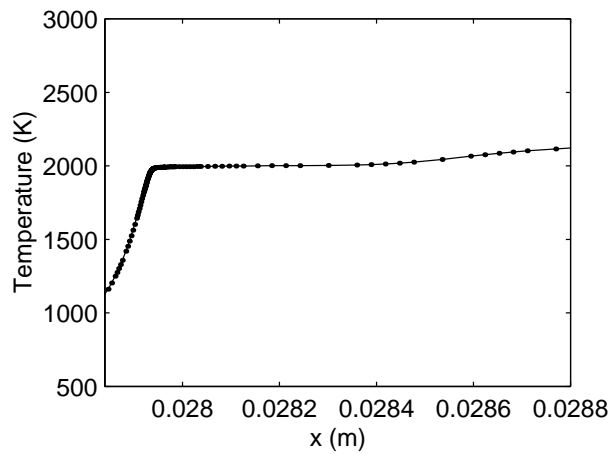
- small entropy layer evident on finer scale,
- temperature rise $\sim 5\text{ K}$; dissipates quickly,
- inviscid calculations before adjustment give persistent temperature rise of $\sim 20\text{ K}$; reaction acceleration small.



Viscous $H_2 - O_2$ Ignition Delay with Wavelets

Close-up: Viscous Shock Structure and Induction Zone

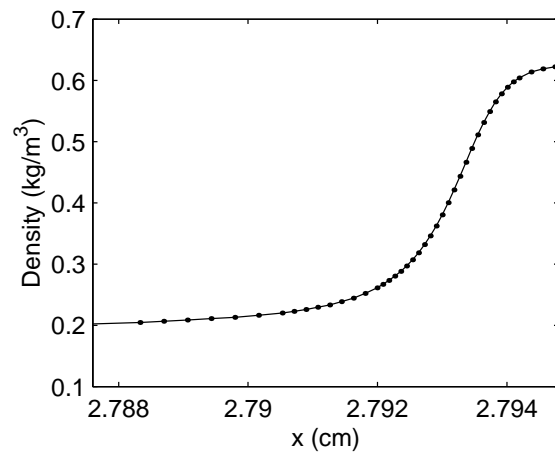
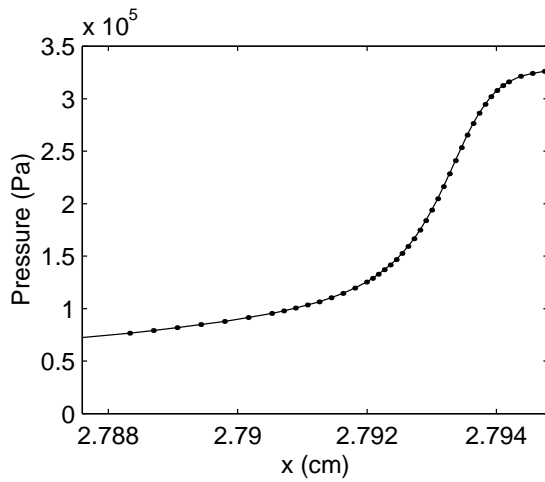
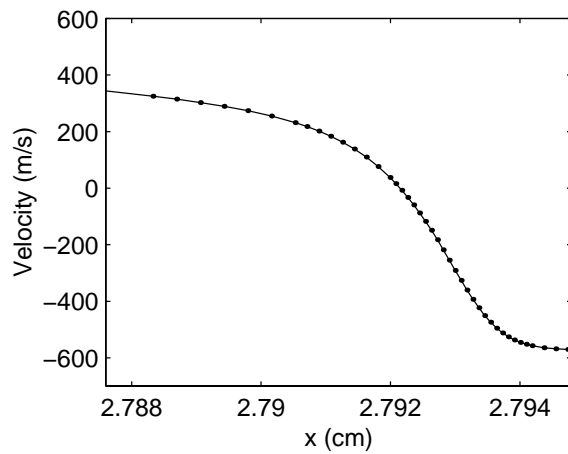
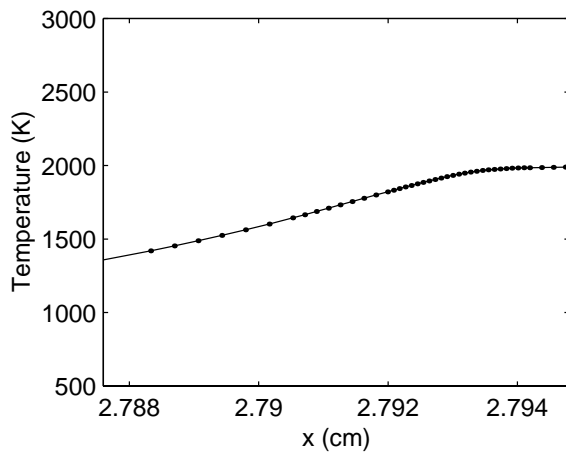
- $t = 230 \mu s$,
- Induction zone length: $\sim 470 \mu m$,
- No significant reaction in viscous shock zone.



Viscous $H_2 - O_2$ Ignition Delay with Wavelets

Closer-up: Viscous Shock Structure Only

- $t = 230 \mu s$
- predicted shock thickness: $\sim 50 \mu m$.

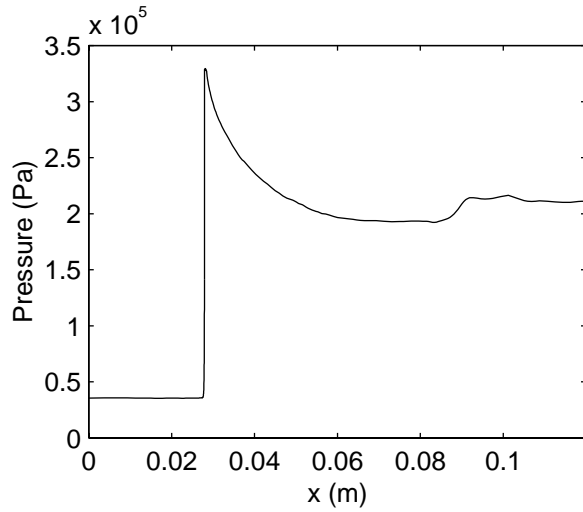


Viscous $H_2 - O_2$ Ignition Delay with Wavelets

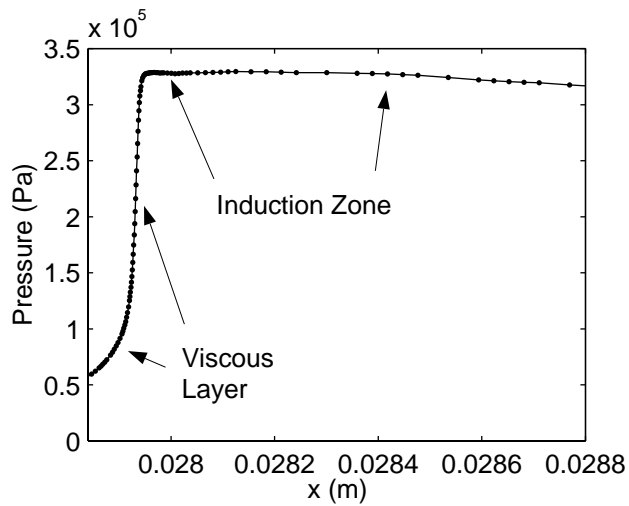
Global and Fine Scale Structures

- $t = 230 \mu s$

Global View

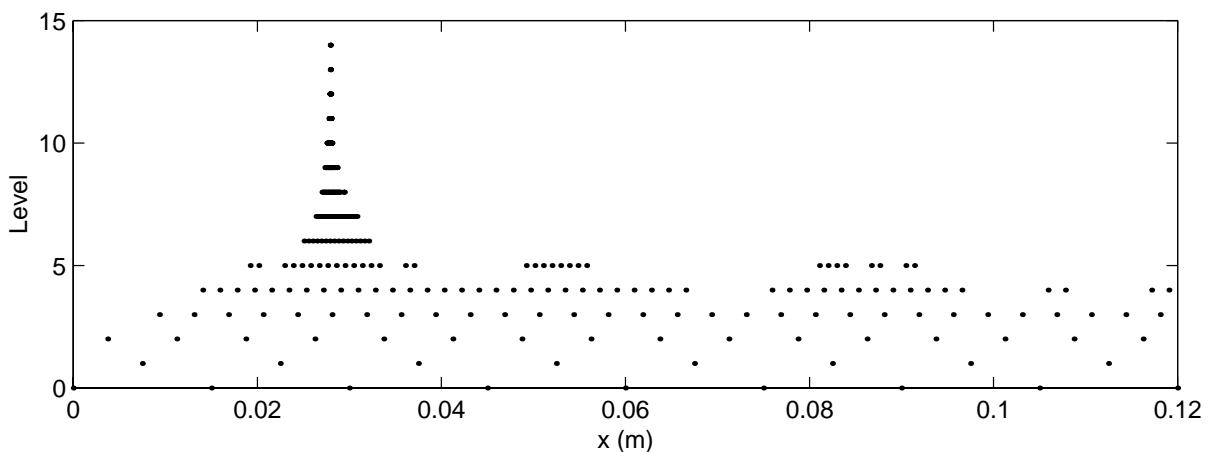
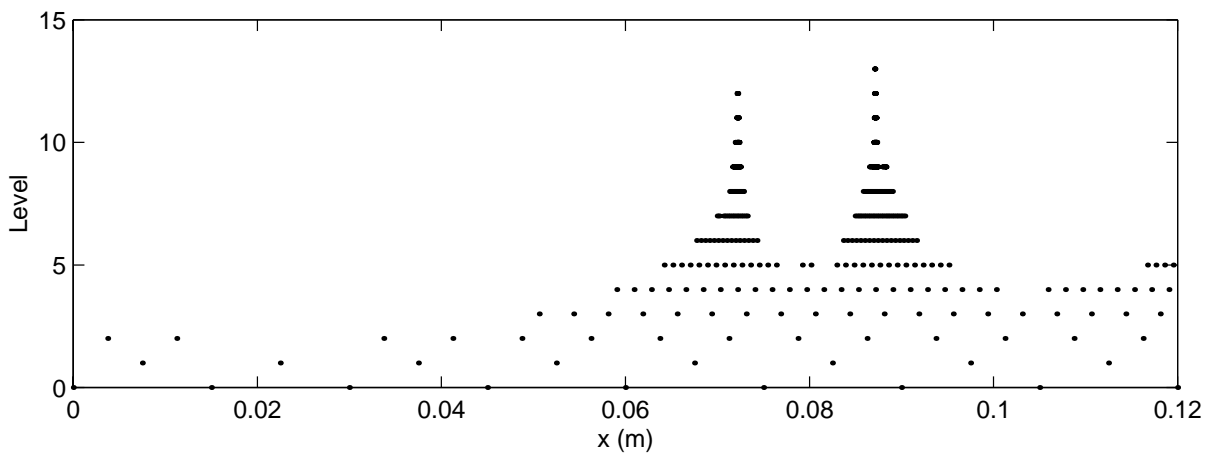


Fine Scale Structure



Viscous $H_2 - O_2$ Ignition Delay with Wavelets, Instantaneous Distributions of Collocation Points

- $t = 180 \mu s$, two-shock structure with consequent collocation point distribution,
- $t = 230 \mu s$, one-shock structure with evolved collocation point distribution.



Application to Gas Phase HMX System

- Simulating isobaric HMX combustion computationally intensive,
- Most effort in solving gas phase convection, reaction, diffusion,
- Based on 45 species, 232 step mechanism of Yetter, et al.,
- Fastest time scales predicted 10^{-16} s (non-physical?),
- Stiffness ratio 10^{11} (vs. 10^9 for $H_2 - O_2$),
- Equations for gas phase combustion of HMX are of form

$$\frac{\partial}{\partial t} \mathbf{q}(x, t) + \frac{\partial}{\partial x} \mathbf{f}(\mathbf{q}(x, t)) = \mathbf{g}(\mathbf{q}(x, t)),$$

- Adiabatic, isobaric,
- Operator splitting appropriate,
- For *non-premixed* problem, higher dimension (≥ 8 !) manifolds necessary!
- Will need to parameterize by ($h, \rho, H, O, N, C, Ar, \geq$ one free parameter)

$$10^7 < h < 10^{11} \text{ erg/g}; 10^{-5} < \rho < 10^{-3} \text{ g/cm}^3; 10^{-32} < \chi_{Ar} < 10^{-2};$$

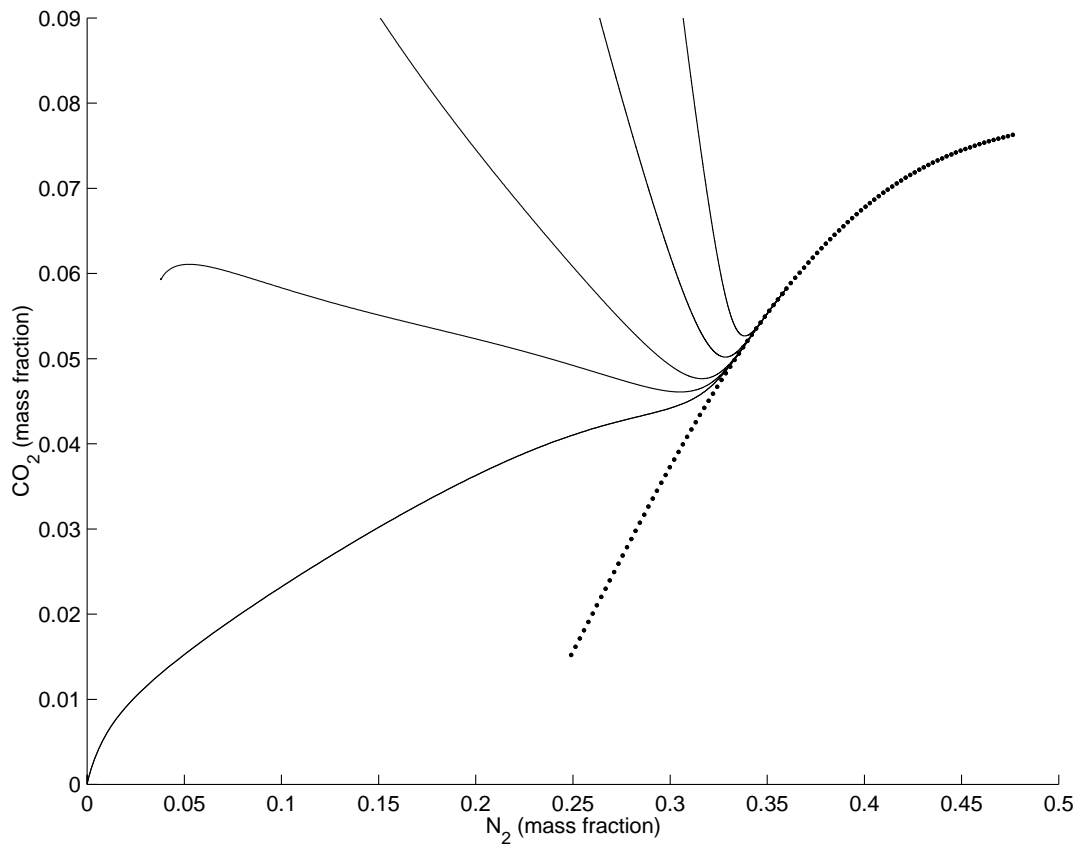
$$0 < \chi_C < 10^1; 0 < \chi_H < 10^1; 0 < \chi_N < 10^1; 0 < \chi_O < 10^1.$$

(Liau, 1999)

- Three-dimensional manifold for preliminary premixed problem?

ILDM for Gas Phase HMX System

- Based on 45 species, 232 step mechanism of Yetter, et al.,
- Adiabatic ($h = 62 \times 10^9 \text{ erg/g}$), isobaric ($P = 32 \text{ bar}$),
- projection in Y_{N_2}, Y_{CO_2} plane.



Conclusions

- Adaptive multilevel wavelet collocation method gives dramatic spatial resolution in viscous one-dimensional H_2/O_2 detonations with detailed kinetics; viscous shocks, entropy layers, and induction zones are resolved,
- Two-dimensional calculations of viscous and inviscid detonations with simple kinetics suggest that physical viscosity is necessary to achieve a converged solution as grid size is reduced,
- Preliminary results on well-stirred systems indicate at least a ten-fold increase in computational efficiency with use of intrinsic low dimensional manifolds,
- Operator splitting allows straightforward implementation of ILDM method in solving PDEs.

Future

- Full coupling of ILDM and wavelet methods soon forthcoming,
- Effort still needed on improving technique of moving onto manifold initially,
- Study of systems with strong interaction of fluid and chemical time scales necessary,
- Detailed studies of efficiency improvement necessary,
- Extensions to multidimensions and complex geometry forthcoming,
- Implementation in parallellized machines to be examined,
- Exercise of method on other realistic test problems forthcoming.